UCRL-16573

Cy. 2 MSd

University of California
Ernest O. Lawrence Radiation Laboratory

SCATTERING OF 40.5 MeV ALPHA-PARTICLES BY C^{12}, C^{13}, N^{14}, N^{15}, O^{16}, AND O^{18}

TWO-WEEK LOAN COPY

This is a Library Circulating Copy which may be borrowed for two weeks. For a personal retention copy, call Tech. Info. Division, Ext. 5545

Berkeley, California

UCRL-16573 Cy 2

DISCLAIMER

This document was prepared as an account of work sponsored by the United States Government. While this document is believed to contain correct information, neither the United States Government nor any agency thereof, nor the Regents of the University of California, nor any of their employees, makes any warranty, express or implied, or assumes any legal responsibility for the accuracy, completeness, or usefulness of any information, apparatus, product, or process disclosed, or represents that its use would not infringe privately owned rights. Reference herein to any specific commercial product, process, or service by its trade name, trademark, manufacturer, or otherwise, does not necessarily constitute or imply its endorsement, recommendation, or favoring by the United States Government or any agency thereof, or the Regents of the University of California. The views and opinions of authors expressed herein do not necessarily state or reflect those of the United States Government or any agency thereof or the Regents of the University of California.

Physical Review

UCRL-16573

UNIVERSITY OF CALIFORNIA

Lawrence Radiation Laboratory
Berkeley, California

AEC Contract No. W-7 05-eng-48

SCATTERING OF 40.5 MeV ALPHA-PARTICLES BY C^{12}, C^{13}, N^{14}, N^{15}, O^{16}, AND O^{18}

B. G. Harvey, J. R. Meriwether, J. Mahoney, A. Bussière de Nercy,
and D. J. Horen

December 1965

SCATTERING OF 40.5 MeV ALPHA-PARTICLES BY C^{12}, C^{13}, N^{14}, N^{15}, O^{16}, AND O^{18}*

B. G. Harvey, J. R. Meriwether, and J. Mahoney,

Lawrence Radiation Laboratory
University of California
Berkeley, California

A. Bussière de Nercy,

Laboratoire Joliot-Curie
Orsay, (S-et-O), France

and D. J. Horen

Naval Radiological Defense Laboratory
San Francisco, California

December 1965

ABSTRACT

Elastic and inelastic scattering of 40.5 MeV α-particles from targets of C^{12}, C^{13}, N^{14}, N^{15}, O^{16}, and O^{18} was studied. Angular distributions were measured for a large number of excited states.

It was found that the shape of the angular distribution depends on the nature of the single particle transition involved. Six examples of quadrupole transitions involving promotion of a $p_{3/2}$ nucleon to the $p_{1/2}$ shell were found. Although the cross sections varied over a tenfold range, the shapes of the angular distributions remained very similar.

Six examples of the dipole transition $p_{1/2} \rightarrow 2s_{1/2}$ and seven examples of the octupole transition $p_{1/2} \rightarrow d_{5/2}$ were also observed. The dipole transitions gave angular distributions of a characteristic and unusual shape.

Excitation of the N^{14} levels at 9.41, 9.71, 10.22, and 10.55 MeV suggests that they are all T=0. The levels at 6.05, 6.70, 7.40, and 7.60 MeV

were not observed: probably they do not exist. A weak level at 10.85 MeV and two strongly excited levels (or groups of levels) at 11.3 and 12.9 MeV were observed in N^{14}.

The angular distribution of particles scattered from the 4.45 MeV level of O^{18} suggests strongly that this level is 1- rather than 3+.

Several unnatural parity states were observed, but no states known to have isotopic spin different from the ground state.

The angular distributions for several scattered particle groups were compared with distorted wave Born approximation calculations and very approximate reduced transition probabilities for excitation of the levels were obtained. For the quadrupole and octupole excitations the results are in reasonably good agreement with values measured by electromagnetic methods.

I. INTRODUCTION

The inelastic scattering of α-particles is a useful method for studying the surface shapes of medium-mass nuclei.[1] The levels most strongly excited are the 2+, 4+, and 3- collective states. It is therefore for the excitation of such levels that most of the angular distributions of scattered particles have been measured. The shapes of the angular distributions are determined by the angular momentum transfer L, while the absolute value of the differential cross section depends upon the collective strength of the level excited.

The light nuclei present many opportunities for studying inelastic scattering of α-particles from targets for which the structure of the initial and final nuclear states is rather well understood. In many cases the transitions should be almost pure single-particle rather than collective. Large numbers of levels are sufficiently well separated in energy to permit resolution of the corresponding groups of scattered particles.

In the present survey experiment, elastic and inelastic scattering of 40.5 MeV α-particles from targets of C^{12}, C^{13}, N^{14}, N^{15}, O^{16}, and O^{18} was studied, using the Berkeley 224-cm (88-inch) spiral ridge cyclotron. The energy was chosen because it is sufficiently high to avoid the worst complications of compound nuclear effects but sufficiently low to permit good energy resolution to be obtained with silicon detectors.

II. EXPERIMENTAL METHOD

The elastic and inelastic scattering of 40.5 ± 0.3 MeV helium ions from the Berkeley 224-cm (88-inch) spiral ridge cyclotron was studied with the equipment that has been previously described.[2] The C^{12} target was a 1.61 mg/cm^2 film made by charring filter paper. Oxygen was removed by heating to about 1400°C in vacuo. The C^{13} target was ethylene gas (C_2H_4) containing 28.9 atom-percent of C^{13}. Considerable decomposition of the ethylene occurred during the course of the measurements, even though the gas pressure in the target cell remained perfectly constant. The cross sections for C^{13} were therefore obtained by reference to the C^{12} peaks in the energy spectra.

The N^{14}, N^{15}, O^{16}, and O^{18} targets were natural N_2 and O_2 gas (for N^{14} and O^{16}) or separated isotopes of 99.9% isotopic purity (N^{15} and O^{18}). The gases were contained in a 7.66 cm diameter cell with a window of Havar* foil 0.00025 cm thick. 1024 channels of a Nuclear Data ND-160 analyzer recorded the pulses from a lithium-drifted silicon detector 1.5 mm thick. The energy resolution ranged from 100 to 300 keV, depending on the scattering angle. It was limited by multiple scattering of α-particles in the Havar windows and in the target gas. This angular dispersion produces a corresponding energy dispersion which is very serious when the energy of scattered particles is a steep function of scattering angle, as it was in the present work. Spectra taken at angles in the vicinity of 25 deg in the laboratory system are shown in Figs. 1, 2, and 3.

---

*Hamilton Watch Company, Waltham, Massachusetts.

III. RESULTS

ENERGY LEVELS OBSERVED

The energies of inelastic groups were measured[2] only with sufficient accuracy to permit identification of the corresponding excited states.

Carbon-12

Scattering of α-particles by C^{12} has been extensively studied.[3-9] The energy levels above about 8 MeV are obscured by a strong continuous spectrum due to four-body break-up, $C^{12}+\alpha \rightarrow 4\alpha$.[10] Except for the very broad 10.1 MeV (0+) level, all known levels up to 14 MeV were observed, including the 0+ level at 7.656 MeV and the unnatural parity (1+) level at 12.71 MeV.

Carbon-13

The scattering of α-particles by C^{13} was observed, but not studied, by Fulbright et al.[11] We observed excitation of levels only below 8 MeV since the continuum from the four-body break-up of C^{12} was very large (70% of the target was C^{12}). No excitation was observed of the levels at 5.51 and 6.10 MeV reported in the reaction $B^{11}(He^3,p)C^{13}$.[12]

Nitrogen-14

In N^{14}, excitation of the first few levels by inelastic scattering of α-particles has been previously reported.[13,14] We observed excitation of many levels up to an excitation of about 13 MeV. No α-groups corresponding to the previously reported[15] levels at 6.70, 7.40, and 7.60 MeV were observed, confirming an earlier suggestion[16] that these levels of N^{14} do not in fact exist. Furthermore, the level at 6.05 MeV reported in the reaction $N^{15}(He^3,\alpha)N^{14}$ (Ref. 17) was not observed.

No known T=1 levels were definitely observed to be excited. A peak corresponding to an excitation of 9.1 MeV is probably due to excitation of the recently found 2- level at 9.129 MeV[18] rather than to excitation of the 9.17 MeV 2+, T=1 level.

Observation of the levels at 9.41, 9.71, 10.22, and 10.55 MeV suggests strongly that they are all T=0.

A weakly excited level was observed at 10.85 MeV and two very strong levels (or groups of levels) at 11.3 and 12.9 MeV. Presumably they also are T=0.

Nitrogen-15

Alpha particle scattering by N^{15} was first studied recently at Berkeley.[19] We have observed excitation of many levels up to 15 MeV but without resolving the higher levels. The level reported at 9.77 MeV[20] was not observed.

Oxygen-16

Scattering of α-particles by O^{16} has been very widely studied[2-5,21-23] for different incident particle energies. Excitation of levels up to 15 MeV was observed in the present work. The unnatural parity 2- level at 8.870 MeV was quite strongly excited. The 0+ excited levels at 6.052 and 11.26 MeV were not observably populated. The 0- levels at 10.925 and 12.798 MeV (whose excitation is forbidden by conservation of spin and parity) were not observed.

Oxygen-18

Many levels below 8 MeV of excitation were observed, but there was no detectable population of the 6.86 MeV level.

ANGULAR DISTRIBUTIONS

Elastic and inelastic angular distributions for C^{12}, C^{13}, N^{14}, N^{15}, O^{16}, and O^{18} are shown in Figs. 4 to 9. The differential cross sections are given in Tables 1-6. Statistical errors were in nearly all cases smaller than random and systematic errors (imperfect measurement of target gas pressure and temperature, errors of background subtraction, difficulties of resolving peaks from one another, and beam integration errors). All these sources of error produced an uncertainty of about ±6% in the cross sections of levels excited with average intensity. For weakly excited or imperfectly resolved levels the errors were naturally much greater, but are very difficult to estimate. The angular uncertainty in all cases is ±0.5 deg, due mainly to multiple scattering in the gas cell windows.

Since it is important in some calculations to know what relative weights to attach to the individual members of a set of measurements, the statistical errors are given for the elastic cross sections in Tables 1-6. The statistical error will measure approximately the relative weights that should be attached to the cross section values.

A computer program was used to make least-squares fits of Gaussian peaks to resolve the individual contributions of imperfectly resolved doublets and triplets in the experimental energy spectra, for instance the 4.91-5.10 MeV and 5.69-5.83 MeV doublets of N^{14}.*

---

*We are indebted to Dr. A. Springer for writing this program.

Carbon-12 (Fig. 4)

The curves for the 4.433 MeV 2+ and 7.656 MeV 0+ levels oscillate clearly out of phase with that of the elastic group, in agreement with the normal Blair phase rule,[1] but the angular distribution for the 2+ level shows no strong oscillations beyond 50 deg.

The oscillatory behavior of the angular distribution for the 9.64 MeV 3- level is unusually weak, but this is perhaps due to the uncertainty in the subtraction of the large background from the four-body break-up. The absence of the first minimum (which would be at about 20 deg in this case) is characteristic of L=3 transitions.

Carbon-13 (Fig. 5)

The angular distribution for the 3.085 MeV 1/2+ level is in phase with that of the elastic group as required by the phase rule for an odd-L transition with change of parity. Previous tests of the phase rule have involved the excitation of more or less collective transitions. Thus it is interesting to observe that the rule is clearly obeyed for this pure single-particle transition.

For the (7.498 - 7.553) MeV unresolved doublet, the negative parity level (7.553 MeV, 5/2-) was responsible for very approximately two-thirds of the combined cross section. The 3.850 MeV 5/2+ level was excited much less strongly than the 3.680 MeV 3/2- level, but it appears to obey the phase rule at small angles.

Nitrogen-14 (Fig. 6)

The 3.945 MeV 1+ and 7.03 MeV 2+ levels give angular distributions that oscillate out of phase with the elastic cross section; their shapes are characteristic of L=2 transitions. The angular distributions for the 4.91 MeV 0-,

5.10 MeV 2-, 5.69 MeV 1- and 5.83 MeV 3- levels are in phase with the elastic angular distribution; these levels are excited by L=1 or L=3 transitions (see below). The 6.21 MeV 1+ level gives rise to an angular distribution very similar in shape to those of the 5.10 and 5.83 MeV negative parity levels. It, and the 6.44 MeV 3+ level, are believed to be excited by a second order process (the differential cross sections are about one-tenth of those for the 5.10 and 5.83 MeV levels).

Nitrogen-15 (Fig. 7)

Angular distributions for the (5.276 MeV 5/2+, 5.304 MeV 1/2+) unresolved doublet, 7.31 MeV 3/2+ and 7.57 MeV 7/2+ levels are in phase with the elastic angular distribution, consistent with the positive parity of all these levels. By comparing the slopes at small angles, and the relative heights of the maxima, we assign an L=1 transition to the 7.31 MeV level and L=3 to the other two. The 8.31 MeV (1/2+ or 3/2+) and 8.57 MeV (5/2+) levels are weakly excited, and while their angular distributions are consistent with a positive parity assignment for these levels, the curves are not accurate enough to give definite information about the L-value for the transitions.

The 6.328 MeV (3/2-) level gives an angular distribution that at small angles looks clearly like an L=2 transition.

Oxygen-16 (Fig. 8)

The cross sections for the 6.131 MeV 3-, 7.115 MeV 1- and 8.870 MeV 2- levels are in phase with the angular distribution of the elastic group, in agreement with their negative parity. Comparison between their curves suggests an L=3 transition for the 6.131 and 8.870 MeV levels and an L=1 transition for the 7.115 MeV level. The 8.870 MeV 2- unnatural parity level is, as expected,[3,22,24] only weakly excited.

Excitation of the 6.916 MeV 2+ level gives an angular distribution that is not exactly out of phase with the elastic cross section, but it is consistent with the positive parity of the level when the curve is contrasted with the angular distributions of the known negative parity levels.

An unresolved group was observed at an excitation of 13.1 MeV but the angular distribution is not plotted in Fig. 8. That we observed excitation of levels at all in this energy region confirms the existence of the 2+, T=0 level recently found at 13.1 MeV.[8]

Oxygen-18 (Fig. 9)

The 5.09 MeV 3-, the (6.34 MeV-6.39 MeV) unresolved doublet and the (7.96 MeV-8.04 MeV-8.08 MeV) unresolved triplet have angular distributions that are in phase with the elastic curve, corresponding to odd-L transitions with a change of parity. The transition is clearly L=3 for excitation of the 5.09 MeV level. The 7.96 MeV and 8.08 MeV members of the triplet seem to be only weakly excited. The angular distributions for the 1.98 MeV and 3.92 MeV 2+ levels are almost exactly out of phase with the elastic angular distribution, confirming the positive parity of the levels. The oscillations of their angular distributions are much stronger than those for any other levels so far observed among the light nuclei: they resemble the angular distributions obtained in the excitation of strongly collective quadrupole levels in somewhat heavier nuclei.

The angular distribution for excitation of the 4.45 MeV level is clearly due to an L=1 transition. The spin of the level must therefore be 1- rather than 3+ or 3-.[25-28]

IV. DISCUSSION

The angular distributions seem to fall into groups depending on the particular dominant single particle transition involved in the excitation. In this respect the angular distributions for excitation of levels in the light nuclei differ from those for excitation of collective levels in heavier nuclei, where the shape of the angular distribution depends almost entirely on the angular momentum transfer, and where the difference between an L=1 or 3 or an L=2 or 4 angular distribution is rather small except at small angles.

$p_{3/2} \rightarrow p_{1/2}$, L=2 Transition

The $p_{3/2} \rightarrow p_{1/2}$ transition might involve a change of 0 or 2 units of angular momentum. If the interaction between an α-particle and a nucleon is spin-independent, the transition will involve only the orbital angular momentum of the nucleon, with no change of spin. The change in the total angular momentum must be $\underset{\sim}{3/2} + \underset{\sim}{1/2} = 1$ or 2 units. Hence in the absence of spin-flip and of parity change, L can only be 2.

Six transitions have been observed that are believed to involve the promotion of a $p_{3/2}$ nucleon into the $p_{1/2}$ shell. In four cases (C^{12} 2+, 4.433 MeV; C^{13} 5/2-, 7.553 MeV; C^{13} 3/2-, 3.680 MeV; and N^{15} 3/2-, 6.328 MeV levels) conservation of angular momentum and parity requires that the excitations be L=2. Since the angular distributions of the scattered α-particles are very much alike in all six cases, it seems quite probable that all six transitions are quadrupole.

Fig. 10 shows the differential cross sections for inelastic scattering of α-particles from the 4.433 MeV 2+ level of C^{12}, the 3.680 MeV 3/2- and 7.553 MeV 5/2- levels of C^{13}, the 3.945 MeV 1+ and 7.03 MeV 2+ levels of N^{14}

and the 6.328 MeV 3/2- level of N^{15} plotted as a function of the parameter $kR\theta = 1/2(k_i+k_f)(1.3\ A^{1/3}+1.2)\theta_{cm}$, where k_i and k_f are the center-of-mass wave numbers of the incident particle and of the outgoing particle at 0 deg. All these levels give rise to angular distributions of about the same shape. Fig. 10 also shows the angular distributions for excitation of the 6.916 MeV 2+ level of O^{16} and the 1.98 MeV and 3.92 MeV 2+ levels of O^{18} for which the shape is quite different.

The shell model components with the largest amplitudes in the wave functions of the 4.433 MeV level of C^{12}, the 3.945 MeV and 7.03 MeV levels of N^{14} and the 6.328 MeV level of N^{15} are: $s^4p^8(p^{-1}_{3/2}\ p_{1/2})_2$,[29] $s^4p^{12}(p^{-1}_{3/2}\ p^{-1}_{1/2})_{1,2}$[30,31] and $s^4p^{12}p^{-1}_{3/2}$[32] respectively. Thus these four levels can be excited by promotion of a $p_{3/2}$ nucleon into the $p_{1/2}$ shell. Since the angular distributions for excitation of the 3.680 MeV 3/2- and 7.553 MeV 5/2- levels of C^{13} resemble those of the other four, these levels of C^{13} should be largely $s^4p^8\left[(p^{-1}_{3/2}\ p_{1/2})_2\ p_{1/2}\right]_{3/2,5/2}$.

The angular distributions for the two 2+ levels of O^{18} and for the 6.916 MeV 2+ level of O^{16} are quite different from the others shown in Fig. 10. Since the $p_{1/2}$ shell is filled in these two nuclei, the promotion $p_{3/2} \rightarrow p_{1/2}$ is impossible. The angular distributions thus seem to be dependent upon the details of the transition and not only upon the angular momentum change.

The configuration given above for the 3/2- and 5/2- levels of C^{13} at 3.680 and 7.553 MeV respectively corresponds to coupling of the $p_{1/2}$ odd neutron to a C^{12} core in the 4.433 MeV 2+ excited state. If the coupling is weak, the angular distributions for the two levels should be similar in shape to that for the excitation of the 2+ state in C^{12}. Further, the reduced transition probabilities, B(E2)↓ of the two C^{13} levels should be equal to that for the 2+ C^{12} level.

The angular distributions for the three levels have roughly the same shape. At the maximum near 40 deg, the sum of the cross sections for the two C^{13} levels is about 11 mb/sr whereas the corresponding C^{12} cross section is 18 mb/sr. The cross sections do not obey either the (2J+1) rule or the center of gravity theorem.[33] The rather large splitting (3.87 MeV) between the two levels shows, of course, that the coupling is in fact rather strong.

$p_{1/2} \rightarrow 2s_{1/2}$, L=1 Transition

The promotion $p_{1/2} \rightarrow 2s_{1/2}$ necessarily involves a dipole transition (L=1). Although there is a general similarity between the inelastic scattering and electric transitions of the same multipole order,[34] there are certain important differences in the special case of a dipole transition.

Protons and neutrons interact in a different way with an electromagnetic field (since their electric charge and magnetic moments are different). The interaction Hamiltonian can therefore be written explicitly in terms of the third component of isospin:

$$H_{int} = - \sum_{i=1}^{A} \left[\frac{e}{2c} \underset{\sim}{v}_i \cdot \underset{\sim}{a}(\underset{\sim}{r}_i) + \frac{1}{2} (\mu_p + \mu_n) \underset{\sim}{\sigma}_i \cdot \underset{\sim}{\mathcal{H}}\right]$$

$$- \sum_{i=1}^{A} \left\{ t_{3_i} \left[\frac{e}{c} \underset{\sim}{v}_i \cdot \underset{\sim}{a}(\underset{\sim}{r}_i) + \frac{1}{2} (\mu_p - \mu_n) \underset{\sim}{\sigma}_i \cdot \underset{\sim}{\mathcal{H}}\right] \right\}$$

$$= H_0 + H_1 \quad .$$

The first sum (H_0) is a scalar in isospin space, but H_1 is the third component of a vector, producing different isospin selection rules. On making a multipole expansion of H_{int}, it is found that H_0 contains almost no E1 part provided that $kR \ll 1$.[35] Electric dipole transitions therefore occur predominantly

through the isospin vector part H_1;H_0 leads only to motion of the nuclear center of mass.

Under the assumption that the particles can be represented by plane waves, and that they interact with the nucleons through a zero-range force, the inelastic scattering operator has the same form as the spin-independent part of the electric operator of the same multipole order.[34] However, under the further assumption that the particles interact identically with protons and neutrons, there will be nothing to correspond to H_1, and hence dipole inelastic scattering excitations will be forbidden provided that $QR \ll 1$ (where Q is the momentum transfer).

Nevertheless, several examples of dipole excitation were observed in the present work. This may be due to breakdown of any of the assumptions mentioned above, but most probably the excitation arises from the failure of the plane wave assumption that is to be expected for strongly-interacting particles such as α-particles.

Excitation through a multiple scattering process is also possible. It has previously been postulated for excitation of the 5.80 MeV 1- level in Ne^{20},[36] by an octupole transition to the 7.17 MeV 3- level followed by a quadrupole transition to the 1- level. The angular distribution for formation of the 1- level was out of phase with the elastic angular distribution, as might be expected for a double transition to a negative parity state. However, of the dipole levels studied in the present work only the 4.45 MeV level of O^{18} gave an anomalous angular distribution. There is as yet no evidence that multiple transitions are involved in excitation of the 7.115 MeV 1- level of O^{16}, even though the strong E3 transition to the 6.131 MeV 3- level[37] and the strong E2 transition from the 3- to the 1- level[38] should make this a particularly favorable case.

Angular distributions of α-particles corresponding to excitation of the 3.085 MeV 1/2+ level of C^{13}, the 4.91 MeV 0- and 5.69 MeV 1- levels of N^{14}, the 7.31 MeV 3/2+ level of N^{15}, the 7.115 MeV 1- level of O^{16} and the 4.45 MeV 1- level of O^{18} are shown in Fig. 11. The differential cross sections are plotted as a function of the parameter $kR\theta$. Except for the 3.085 MeV level of C^{13}, for which the data are poor at small angles, the angular distributions have a very characteristic and unusual shape—there is little or no decrease in cross section between the first and second maxima. The shell model components with the largest amplitudes for these levels are: $s^4p^8s_{1/2}$(3.085 MeV, C^{13}),[39] $s^4p^8(p_{1/2}\ s_{1/2})_{0,1}$, (4.91 MeV and 5.69 MeV, N^{14}),[30,31] $s^4p^{12}\left[(p^{-1}_{1/2}\ s_{1/2})_1 p^{-1}_{1/2}\right]_{3/2}$ (7.31 MeV, N^{15})[32] and $s^4p^{12}(p^{-1}_{1/2}\ s_{1/2})_1$ (7.115 MeV, O^{16}).[29,40] Thus these excited states can be formed by the single-nucleon transition $p_{1/2} \rightarrow 2s_{1/2}$.

Sebe[39] has calculated wave functions for the positive parity levels of C^{13}, assuming that the odd neutron can be in the $2s_{1/2}$, $1d_{5/2}$, or $1d_{3/2}$ shell model states coupled to a C^{12} core that can be either in the 0+ ground state or in the 2+ 4.433 MeV state. According to this model, the 3.085 MeV 1/2+ state is almost pure $2s_{1/2}$ with the C^{12} core in the ground state. The 6.860 MeV 5/2+ level of C^{13} is only weakly excited at most angles, consistent with Sebe's wave function, according to which excitation both of the C^{12} core and of the odd neutron would be required. The 3.850 MeV 5/2+ level should be excited quite readily by a $p_{1/2} \rightarrow d_{5/2}$ transition of the odd neutron, but for some reason the peak is apparently only a minor component of the 3.680-3.850 MeV unresolved doublet. The positive parity levels of C^{13} can be formed only by excitation of p-shell nucleons into the sd shell, whereas the negative parity levels can be formed by processes related to the very strong excitation of the C^{12} 4.433 MeV quadrupole level.

In earlier experiments with 65 MeV alpha particles,[2] the characteristic L=1 shape observed in the present work for the angular distribution corresponding to excitation of the 7.115 MeV 1- level of O^{16} was not observed. Its angular distribution differed from the L=3 shape only in the absence of a sharp peak at 20°.

$p_{1/2} \rightarrow d_{5/2}$ L=3 Transition

The promotion of a $p_{1/2}$ nucleon to the $d_{5/2}$ shell could involve an orbital angular momentum transfer of 1 or 3 units. Seven examples of this transition have been identified: some of them are required by angular momentum and parity conservation to be L=3 (e.g., the excitation of the 6.131 MeV 3- level of O^{16}). The similarity of the seven angular distributions suggests that these transitions are all octupole.

Figure 12 shows the angular distributions of α-particles scattered from the 5.10 MeV 2- and 5.83 MeV 3- levels of N^{14}, the 5.276 MeV 5/2+ and 7.57 MeV 7/2+ levels of N^{15}, the 6.131 MeV 3- and 8.870 MeV 2- levels of O^{16} and the 5.09 MeV 3- level of O^{18}. The shell model components with the largest amplitudes in the wave functions of these levels are: $s^4p^8(p_{1/2}\ d_{5/2})_{2,3}$ (N^{14}, 5.10 and 5.83 MeV),[30,31] $s^4p^8\left[(p_{1/2}\ d_{5/2})_3 p_{1/2}\right]_{5/2,7/2}$ (N^{15}, 5.276 and 7.57 MeV),[32] and $s^4p^{12}(p_{1/2}^{-1}\ d_{5/2})_{2,3}$ (O^{16}, 8.870 and 6.131 MeV).[29,40] Thus the most important single particle transition in the excitation of these levels should be $p_{1/2} \rightarrow d_{5/2}$.

In the case of the 8.870 MeV 2- level of O^{16}, either octupole or dipole excitation would have to be accompanied by a spin-flip, so it is perhaps surprising that at small angles the angular distribution resembles rather closely those of the non-spin-flip transitions, although at larger angles substantial differences are observed. The differential cross section for formation

of the 2- level begins to rise at large angles: this behavior is characteristic of the more complex excitation processes. In scattering experiments at 65 MeV,[2] excitation of the 2- level gave an angular distribution that seemed closer to the L=1 shape than to L=3.

In an earlier publication,[19] the excitation of the 5.276 and 7.57 MeV levels of N^{15} was considered as an example of weak coupling of an odd nucleon (in this case a $p_{1/2}$ proton hole) to an octupole core vibration, the core in this instance being O^{16}. The octupole reduced transition probabilities, $B(E3)\downarrow/e^2$, were found to be nearly equal for these two levels in N^{15} to that for the 6.131 MeV octupole state of O^{16}. The weak coupling model appears to give a better account of these octupole states that it did for the quadrupole levels of C^{13} discussed above. The coupling is in fact somewhat weaker in N^{15}: the splitting is only 2.29 MeV compared with 3.87 MeV in C^{13}.

In addition to the octupole levels, one might expect to find in N^{15} doublets of levels based on the strongly excited 1- and 2+ levels of O^{16}. The 1/2+ and 3/2+ levels of N^{15} at 5.304 and 7.31 MeV are possible candidates for the dipole doublet. The 5.304 MeV level was not resolved in the present work; the 7.31 MeV level, however, does give an angular distribution similar to that of the 7.115 MeV 1- level of O^{16}.

The only quadrupole level found in N^{15} (the 6.328 MeV 3/2- level) appears to be related to the $p_{3/2} \rightarrow p_{1/2}$ single particle transition rather than to the 6.916 MeV 2+ level of O^{16}.

The L=3 excitation of the 3- level of C^{12} gives an angular distribution markedly different from the octupole excitations considered in the present section. In C^{12}, the single particle transition with the largest amplitude is $p_{3/2} \rightarrow d_{5/2}$ rather than $p_{1/2} \rightarrow d_{5/2}$.[29] As in the case of the quadrupole

levels discussed above, the detailed shape of an octupole angular distribution seems to depend on the details of the transition as well as on the angular momentum transfer.

Two-Nucleon Transitions

Several transitions, corresponding to the promotion of two nucleons from one shell into another were observed.

In C^{12}, the 7.656 MeV 0+ level is excited with surprising strength, considering that it can be populated only by the promotion of two or four nucleons from the $p_{3/2}$ ground state into the higher shells. The strong excitation of the C^{12} 4.433 MeV 2+ level shows that the individual $p_{3/2} \rightarrow p_{1/2}$ quadrupole transitions are collectively enhanced.

The configurations $s^4p^8(s_{1/2})^2_1$ and $s^4p^8(s_{1/2}\ d_{5/2})_3$ of the 6.21 and 6.44 MeV levels of $N^{14\ 31}$ require that these states be formed from the ground state through the two-nucleon promotions $(p_{1/2} \rightarrow 2s_{1/2})^2$ and $(p_{1/2} \rightarrow 2s_{1/2})$ $(p_{1/2} \rightarrow d_{5/2})$. The cross sections are indeed rather small, as are those for formation of the 8.99 MeV 1+ $s^4p^{12}(p_{3/2})^{-2}_1$ and 8.963 MeV 5+ $s^4p^8(d_{5/2})^2_5$ levels, which could be populated through the transitions $(p_{3/2} \rightarrow p_{1/2})^2$ and $(p_{1/2} \rightarrow d_{5/2})^2$.

V. REDUCED TRANSITION PROBABILITIES

Comparison of experimental cross sections with distorted wave Born approximation (DWBA) calculations permits the extraction of reduced transition probabilities. The potential used in the present work was of the form:

$$V = V_c - V_R \left[1+\exp\left(\frac{r-R}{a}\right)\right]^{-1} + iW \left[1+\exp\left(\frac{r-R}{b}\right)\right]^{-1}$$

where V_c, V_R, and W are the Coulomb, real and imaginary parts of the potential respectively. The parameters a and b are related to the diffuseness of the real and imaginary potentials.

The appropriate values of the parameters V_R, W, a and b were obtained from an optical model analysis of the elastic angular distribution, using a computer program described by R. H. Pehl.[41] Reasonably good fits to the experimental elastic angular distributions were obtained with the parameters shown in Table 7. As a typical example, Fig. 13 shows the calculated and experimental elastic angular distributions for N^{15}.

With the parameters shown in Table 7, and using a derivative Woods-Saxon nuclear form factor, inelastic angular distributions were calculated in DWBA. The calculated angular distributions were never a particularly good fit to the experimental results: probably more detailed calculations with microscopic wave functions are needed, although results of some preliminary attempts were not particularly encouraging. Nevertheless, comparison of the calculated and experimental angular distributions was made in order to extract extremely approximate values of the reduced quadrupole and octupole transition probabilities connecting the target ground state and each excited state. The values thus obtained are given in Tables 8 and 9. Two fairly typical comparisons of calculated and experimental angular distributions are shown in Figs. 14 and 15.

As Table 8 shows, the present experiment yielded values for the reduced electric quadrupole transition probabilities $B(E2)\downarrow/e^2$ in surprisingly good agreement with values obtained by other workers by electromagnetic measurements

(except for the 3.92 MeV level of O^{18}). The $B(E3)\downarrow/e^2$ values of Table 9 are lower by a factor of about 2 than the three electromagnetic results.

In view of the profound difference between the inelastic scattering dipole operator and the electric dipole operator, there is little point in comparing the inelastic scattering dipole transition probabilities with the electromagnetic values, especially since the use of a collective nuclear model for the distorted wave calculations makes little sense for the dipole states. Nevertheless, it is interesting that the inelastic scattering cross sections for excitation of the 7.115 MeV and 4.45 MeV 1- levels of O^{16} and O^{18} are respectively 10^4 and 10^6 times greater than would be expected from the electromagnetic dipole transition probabilities!

For the self-conjugate nucleus O^{16}, the isospin vector part H_1 of the electromagnetic Hamiltonian vanishes, so apart from the differences due to the greater absorption of α-particles (and therefore greater departure from the plane wave approximation) the inelastic scattering and electromagnetic transitions should be formally similar. That they are not is presumably due to the very great distortion of the α-particle waves.

The DWBA calculation gave an angular distribution for excitation of the 4.45 MeV 1- level of O^{18} that was in very poor agreement with the experimental results. Figure 11 shows that although the angular distribution for this level has the equal maxima that seem to be characteristic of the dipole transitions, the values of $kR\theta$ at which they fell are substantially lower than for any other of the dipole excitations. As already mentioned, double excitation through the 5.09 MeV 3- level might be important.

Further studies of the very interesting dipole excitations are in progress.

ACKNOWLEDGMENTS

We wish to thank the operating staff of the spiral ridge cyclotron and the machine shop personnel for the extremely efficient operation of the machine. Roy Burton was responsible for the elegant design of most of the scatter chamber equipment. F. S. Goulding and his Chemistry Electronics Support Group provided the excellent silicon detectors and the electronics. We enjoyed many very helpful discussions with Professors J. S. Blair and H. McManus, but especially with Dr. N. K. Glendenning.

One of us (A. B. de N.) would like to acknowledge the hospitality of the 88-inch cyclotron group of the Lawrence Radiation Laboratory.

FOOTNOTES AND REFERENCES

*This work was supported by the U. S. Atomic Energy Commission and BUSHIPS.

1. J. S. Blair, Phys. Rev. 115, 928 (1959).
2. B. G. Harvey, E. J.-M. Rivet, A. Springer, J. R. Meriwether, W. B. Jones, J. H. Elliott, and P. Darriulat, Nucl. Phys. 52, 465 (1964).
3. J. C. Corelli, E. Bleuler and D. J. Tendam, Phys. Rev. 116, 1184 (1959).
4. A. I. Yavin and G. W. Farwell, Nucl. Phys. 12, 1 (1959).
5. J. Aguilar, W. E. Burcham, J. Catala, J. B. A. England, J. S. C. McKee, and J. Rotblat, Proc. Royal Soc. (London) 254A, 395 (1960).
6. G. B. Shook, Phys. Rev. 114, 310 (1959).
7. T. Mikumo, H. Yamaguchi, I. Nonaka, M. Odera, Y. Hashimoto, M. Kondo, and T. Maki, J. Phys. Soc. Japan 15, 1158 (1960), and unpublished reports, INSJ 60 and INSJ 61 (August 1963), Institute for Nuclear Studies, Tokyo.
8. G. E. Mitchell, E. B. Carter, and R. H. Davis, Phys. Rev. 133, B1434 (1964); I. V. Mitchell and T. R. Ophel, Nucl. Phys. 66, 553 (1965).
9. I. M. Naqib, Thesis, University of Washington, (1962).
10. L. B. Brown and H. B. Knowles, Phys. Rev. 125, 1339 (1962).
11. H. W. Fulbright, N. O. Lassen, and N. O. Roy Poulsen, Kgl. Danske Videnskab. Selskab, Mat.-Fys. Medd. 31, No. 10 (1959).
12. C. D. Moak, A. Galonsky, R. L. Traughber, and C. M. Jones, Phys. Rev. 110, 1369 (1958).
13. W. D. Ploughe, Phys. Rev. 122, 1232 (1961).
14. I. Nonaka, T. Mikumo, H. Yamaguchi, S. Hitaka, T. Maki, T. Nakashima and M. Mukae, unpublished report INSJ 57 (May 1963), Institute for Nuclear Studies, Tokyo.

15. T. Lauritsen and F. Ajzenberg-Selove, Energy Levels of the Light Nuclei, Nuclear Data Sheets, May 1962.

16. R. E. Brown, Astrophys. J. 137, 338 (1963).

17. D. D. Clayton, Phys. Rev. 128, 2254 (1962).

18. R. W. Detenbeck, J. C. Armstrong, A. S. Figuera, and J. B. Marion, University of Maryland Technical Report 438, February 1965.

19. A. Bussière, N. K. Glendenning, B. G. Harvey, J. Mahoney, J. R. Meriwether, and D. J. Horen, Phys. Letters 16, 296 (1965).

20. R. Chiba, Phys. Rev. 123, 1316 (1961).

21. J. C. Jodogne, P. C. Macq, and J. Steyaert, Phys. Letters 2, 325 (1963).

22. J. Kokame, K. Fukunaga, N. Inoue, and H. Nakamura, Phys. Letters 8, 342 (1964).

23. I. Nonaka, T. Mikumo, H. Yamaguchi, S. Hitaka, T. Maki, T. Nakashima, and M. Mukae, unpublished report INSJ 56 (May 1963), Institute for Nuclear Studies, Tokyo.

24. W. W. Eidson and J. G. Cramer, Phys. Rev. Letters 9, 497 (1962).

25. S. Hinds and R. Middleton, in Proc. Rutherford Jubilee International Conf., Manchester, 1961 (Heyward, London, 1961).

26. A. A. Jaffe, F. de S. Barros, P. D. Forsyth, J. Muto, I. J. Taylor, and S. Ramavataram, Proc. Phys. Soc. (London) 76, 914 (1960).

27. K. Yagi, Y. Nakajima, K. Katori, Y. Awaya and M. Fujioka, Nucl. Phys. 41, 584 (1963).

28. R. Middleton and D. J. Pullen, Nucl. Phys. 51, 63 (1964).

29. V. Gillet and N. Vinh Mau, Nucl. Phys. 54, 321 (1964).

30. E. K. Warburton and W. T. Pinkston, Phys. Rev. 118, 733 (1960).

31. W. W. True, Phys. Rev. 130, 1530 (1963).

32. E. C. Halbert and J. B. French, Phys. Rev. 105, 1563 (1957).

33. R. D. Lawson and J. L. Uretsky, Phys. Rev. 108, 1300 (1957).

34. W. T. Pinkston and G. R. Satchler, Nucl. Phys. 27, 270 (1961).

35. H. A. Bethe, Rev. Mod. Phys. 9, 69 (1937).

36. A. Springer and B. G. Harvey, Phys. Rev. Letters 14, 316 (1965).

37. T. K. Alexander and A. E. Litherland, Chalk River Report PR-P-64 (1964).

38. S. Gorodetzky, P. Mennrath, W. Benenson, P. Chevallier, and F. Scheibling, J. Phys. (Paris) 24, 887 (1963).

39. T. Sebe, Progr. Theoret. Phys. (Kyoto) 30, 290 (1963).

40. J. P. Elliott and B. H. Flowers, Proc. Roy. Soc. (London) 242, 57 (1957).

41. R. H. Pehl, (Ph.D. Thesis) University of California Lawrence Radiation Laboratory Report, UCRL-10993 (1963).

42. S. Devons, Proc. Conf. on Electromagnetic Lifetimes and Properties of Nuclear States, NAS-NCR Publication No. 974 (1962).

43. G. R. Bishop, M. Bernheim and P. Kossanyi-Demay, Nucl. Phys. 54, 353 (1964).

44. C. P. Swann and F. R. Metzger, Phys. Rev. 108, 982 (1957).

45. A. E. Litherland, M. J. L. Yates, B. M. Hinds, and D. Eccleshall, Nucl. Phys. 44, 220 (1963).

46. F. Lacoste and G. R. Bishop, Nucl. Phys. 26, 511 (1961).

47. M. A. Eswaran and C. Broude, Can. J. Phys. 44, 1311 (1964).

FIGURE CAPTIONS

Fig. 1. Energy spectra of 40.5 MeV α-particles scattered from C^{12} (upper) and C^{13} (lower).

Fig. 2. Energy spectra of 40.5 MeV α-particles scattered from N^{14} (upper) and N^{15} (lower).

Fig. 3. Energy spectra of 40.5 MeV α-particles scattered from O^{16} (upper) and O^{18} (lower).

Fig. 4. Angular distributions for elastic and inelastic scattering of 40.5 MeV α-particles by C^{12}.

Fig. 5. Angular distributions for elastic and inelastic scattering of 40.5 MeV α-particles by C^{13}.

Fig. 6. Angular distributions for elastic and inelastic scattering of 40.5 MeV α-particles by N^{14}.

Fig. 7. Angular distributions for elastic and inelastic scattering of 40.5 MeV α-particles by N^{15}.

Fig. 8. Angular distributions for elastic and inelastic scattering of 40.5 MeV α-particles by O^{16}.

Fig. 9. Angular distributions for elastic and inelastic scattering of 40.5 MeV α-particles by O^{18}.

Fig. 10. L=2 angular distributions for inelastic scattering of 40.5 MeV α-particles.

Fig. 11. L=1 angular distributions for inelastic scattering of 40.5 MeV α-particles.

Fig. 12. L=3 angular distributions for inelastic scattering of 40.5 MeV α-particles.

Fig. 13. Optical model fit to elastic scattering of 40.5 MeV α-particles by N^{15}.

Fig. 14. Distorted Wave Born Approximation (DWBA) angular distribution for excitation of the 6.916 MeV 2+ level of O^{16} by inelastic scattering of 40.5 MeV α-particles. (The fit is representative of the worst results).

Fig. 15. Distorted Wave Born Approximation (DWBA) angular distribution for excitation of the 5.276 MeV 5/2+ level of N^{15} by inelastic scattering of 40.5 MeV α-particles. (The fit is representative of the best results).

Table I. C^{12}.

E_α = 40.5 MeV

Elastic 0+ Level			4.433 MeV 2+ Level		7.656 MeV 0+ Level		9.64 MeV 3- Level	
θ_{cm}	$d\sigma/d\Omega$ (mb/sr)	Stat. Error (mb/sr)	θ_{cm}	$d\sigma/d\Omega$ (mb/sr)	θ_{cm}	$d\sigma/d\Omega$ (mb/sr)	θ_{cm}	$d\sigma/d\Omega$ (mb/sr)
10.8	4128	16.5					11.4	30.1
13.5	1593	6.4					14.2	22.5
16.1	328	2.6	16.5	44.3			17.0	25.6
18.8	84.4	4.3	19.2	46.6	19.5	3.73	19.8	18.2
21.4	81.2	1.4	21.9	35.7	22.3	2.57	22.6	14.0
24.1	190	2.1	24.6	22.2	25.0	0.845	25.4	11.0
26.7	208	1.7	27.3	13.9	27.8	0.403	28.1	8.87
29.3	130	1.2	30.0	11.4	30.5	0.899	30.9	6.84
32.0	52.9	0.37	32.6	13.6	33.2	2.37	33.7	6.21
34.6	8.15	0.15	35.3	16.8	35.9	3.00	36.4	6.62
37.2	1.87	0.07	37.9	17.2	38.6	2.64	39.1	7.24
39.8	14.1	0.20	40.6	15.3	41.3	1.37	41.9	7.80
42.4	25.8	0.26	43.2	11.0	44.0	0.438	44.6	6.65
44.9	28.2	0.28	45.9	8.28	46.7	0.276	47.3	5.63
47.5	20.8	0.17	48.5	6.43	49.3	0.716	50.0	4.83
50.1	12.5	0.12	51.2	4.97	52.0	1.21	52.6	4.12
52.6	7.25	0.10	53.6	4.89	54.6	1.40	55.3	3.66
55.1	7.22	0.10	56.2	4.64	57.2	1.32	57.9	3.55
57.6	10.5	0.13	58.7	4.22	59.8	0.823	60.6	3.60
60.1	15.5	0.15	61.3	3.89	62.4	0.546	63.2	3.18
62.6	17.5	0.16	63.8	3.78	64.9	0.517	65.7	2.71
65.0	14.8	0.10	66.3	3.69	67.4	0.846	68.3	2.26
65.0	16.4	0.21	71.8	4.30	72.4	1.21	73.3	1.42
74.7	4.35	0.08	76.1	5.20	77.4	0.813	78.3	1.96
79.4	3.08	0.07	80.8	7.30	82.2	0.652	83.2	2.22
84.0	1.72	0.05	85.5	5.56	86.9	0.499		

Table II. C^{13}.

E_α = 40.5 MeV

Elastic 1/2-			3.085 MeV 1/2+		3.680 MeV 3/2-		3.850 MeV 5/2+		7.498 + 7.553 MeV 7/2+ 5/2-	
θ_{cm}	$d\sigma/d\Omega$ (mb/sr)	Stat. Error (mb/sr)	θ_{cm}	$d\sigma/d\Omega$ (mb/sr)	θ_{cm}	$d\sigma/d\Omega$ (mb/sr)	θ_{cm}	$d\sigma/d\Omega$ (mb/sr)	θ_{cm}	$d\sigma/d\Omega$ (mb/sr)
19.7	11.4	0.47			20.0	4.75	20.1	14.8	24.5	4.59
21.0	58.8	1.12			21.4	4.45	21.4	10.7	27.2	2.86
23.6	132	0.92			24.0	2.41	24.0	6.77	29.8	2.69
26.2	153	6.27	26.5	3.26	26.6	1.67	26.6	4.4	32.5	2.98
28.8	109	2.62	29.2	1.32	29.2	2.77	29.3	1.56	36.5	4.52
28.8	98.0	0.78	31.8	0.52	31.9	3.53	31.9	0.59	37.8	4.23
31.3	34.7	3.4	34.4	0.54	34.5	4.19	34.5	0.49	37.8	4.49
31.3	43.9	0.53	35.7	0.81	35.8	4.64	35.8	0.80	40.4	4.75
33.9	8.47	0.20	37.0	0.87	37.0	5.03	37.1	0.43	43.1	4.17
35.2	2.32	0.11	37.0	0.98	37.0	4.18	37.1	1.26	45.7	3.28
36.5	9.68	0.22	39.5	1.43	39.6	4.69	39.7	1.52	47.0	3.09
36.5	12.1	0.28	42.1	1.08	42.2	4.19	42.2	1.22	49.5	2.04
39.0	20.3	0.37	44.7	0.93	44.8	3.71	44.8	0.93	53.4	1.95
41.6	27.1	0.43	45.9	0.55	46.0	3.17	46.1	0.23	54.7	2.04
44.1	28.1	0.39	48.5	0.29	48.6	2.24	48.6	0.60	56.0	1.70
45.3	23.3	0.49	52.2	0.21	52.4	2.01	52.4	0.10	58.5	1.53
45.3	20.4	1.37	53.5	0.26	53.6	1.96	53.7	0.19	61.0	1.75
47.9	14.7	0.46	54.7	0.24	54.9	1.86	54.9	0.29	63.5	1.72
51.5	10.1	0.23	57.2	0.32	57.4	1.71	57.4	0.11	66.0	1.69
52.9	10.6	0.21	59.7	0.30	59.9	2.06	59.9	0.15	68.5	1.89
54.1	11.0	0.23	62.2	0.23	62.3	1.72	62.4	0.17	70.9	2.02
56.6	11.4	0.21	67.0	0.15	64.8	1.42	64.8	0.18	73.4	1.80
59.0	15.1	0.41	69.4	0.31	67.2	1.20	67.2	0.57	75.8	1.63
61.4	15.0	0.41	71.8	0.34	69.6	1.58	69.7	0.09		
63.9	13.3	2.5	74.2	0.41	72.0	0.82	72.0	1.04		
66.3	12.1	0.16			74.4	2.20				
68.6	8.54	0.20								
71.0	5.82	0.17								
73.4	3.89	0.19								

Table III. N^{14}.

E_α = 40.5 MeV

Elastic 1+ Level			3.945 MeV 1+ Level		4.91 MeV 0- Level		5.10 MeV 2- Level		5.69 MeV 1- Level		5.83 MeV 3- Level		6.21 MeV 1+ Level		6.44 MeV 3+ Level		7.03 MeV 2+ Level	
θ_{cm}	dσ/dΩ (mb/sr)	Stat. Error (mb/sr)	θ_{cm}	dσ/dΩ (mb/sr)	θ_{cm}	dσ/dΩ (mb/sr)	θ_{cm}	dσ/dΩ (mb/sr)	θ_{cm}	dσ/dΩ (mb/sr)	θ_{cm}	dσ/dΩ (mb/sr)	θ_{cm}	dσ/dΩ (mb/sr)	θ_{cm}	dσ/dΩ (mb/sr)	θ_{cm}	dσ/dΩ (mb/sr)
7.7	2181.5	13.3	18.3	1.43	15.7	0.434	15.7	3.29	15.8	0.228	15.8	4.89	17.1	.519	17.2	.908	18.5	0.407
10.4	3896.5	9.64	18.4	1.23	17.0	0.454	17.1	3.80	17.1	0.398	17.1	5.28	18.4	.349	18.5	.592	18.5	1.21
11.7	2450.5	20.0	20.9	0.967	18.3	0.119	18.4	3.51	18.4	0.215	18.4	4.78	18.4	.644	18.5	.919	21.2	0.546
12.9	1672	14.6	20.9	0.793	18.3	0.387	18.4	4.53	18.4	0.385	18.4	5.82	21.1	.327	21.1	.441	21.2	0.972
13.0	1368.1	19.2	23.5	0.480	21.0	0.471	21.0	3.48	21.0	0.231	21.0	4.98	21.1	.476	21.1	.819	23.8	0.436
13.0	2460.9	12.0	23.5	0.436	21.0	0.357	21.0	4.60	21.0	0.358	21.0	6.41	23.7	.193	23.7	.360	23.8	0.457
15.4	367	2.31	26.1	0.329	23.6	0.650	23.6	2.54	23.6	0.492	23.6	3.86	23.7	.270	23.7	.557	26.4	0.502
15.5	269	1.34	26.2	0.579	23.6	0.785	23.6	3.25	23.6	0.363	23.6	5.56	26.3	.231	26.3	.480	26.4	0.474
16.8	72.8	0.84	28.6	0.721	26.1	0.890	26.2	1.99	26.2	0.739	26.3	3.16	26.3	.208	26.3	.432	26.4	0.478
18.0	15.2	0.16	28.8	0.770	26.1	0.732	26.2	2.31	26.2	0.384	26.3	4.07	28.9	.227	28.9	.307	29.0	0.561
18.1	10.37	0.14	31.6	1.04	28.7	0.625	28.8	1.29	28.8	0.658	28.9	2.09	28.9	.184	28.9	.316	29.0	0.537
20.5	73.2	1.19	31.8	1.036	28.7	0.466	28.8	1.42	28.8	0.157	28.9	2.66	31.5	.156	31.5	.198	31.6	0.734
20.6	77.8	0.41	33.8	1.39	31.3	0.656	31.3	0.809	31.4	0.209	31.4	1.50	31.5	.165	31.5	.216	31.6	0.774
23.1	163.1	0.40	33.9	1.34	31.3	0.525	31.3	0.774	31.4	0.161	31.5	1.47	34.1	.135	34.1	.224	34.2	0.854
23.1	174	0.62	36.3	1.39	33.9	0.805	33.9	0.834	34.0	0.352	34.0	1.22	34.1	.159	34.1	.171	34.2	0.883
25.7	178	0.49	36.4	1.38	33.9	0.518	33.9	0.870	34.0	0.512	34.0	1.02	36.7	.161	36.7	.228	36.8	0.935
25.8	181.9	0.67	38.9	1.16	36.5	1.08	36.5	1.04	36.6	0.595	36.6	1.79	36.7	.182	36.7	.151	36.8	0.872
25.8	158.9	0.94	39.0	1.31	36.5	0.748	36.5	0.948	36.6	0.917	36.6	1.16	39.2	.221	39.3	.117	39.4	0.804
25.8	155.7	0.59	41.4	1.03	39.0	1.17	39.0	1.19	39.1	1.03	39.2	1.42	39.2	.188	39.3	.174	39.4	0.835
28.2	112	0.32	41.5	0.999	39.0	0.913	39.0	1.05	39.1	0.833	39.2	1.71	41.8	.150	41.8	.230	42.0	0.533
28.3	84.2	0.58	43.9	0.830	41.5	0.945	41.6	0.649	41.7	1.38	41.7	0.924	41.8	.189	41.8	.129	42.0	0.676
28.3	106.1	0.53	44.0	0.800	41.5	0.998	41.6	0.941	41.7	1.83	41.7	1.92	44.3	.168	44.4	.158	42.0	0.760
30.7	40.5	0.20	46.4	0.630	41.5	0.855	41.6	0.926	41.7	0.843	41.7	1.87	44.3	.152	44.4	.104	44.5	0.607
30.9	36.25	0.23	46.5	0.603	44.1	0.625	44.1	0.737	44.2	0.957	44.3	1.43	46.9	.116	46.9	.168	44.5	0.567
33.3	8.39	0.097	48.9	0.550	44.1	0.696	44.1	0.678	44.2	0.706	44.3	1.60	46.9	.117	46.9	.108	47.0	0.500
33.4	6.80	0.085	49.0	0.509	46.6	0.449	46.6	0.395	46.8	0.562	46.8	0.951	49.4	.180	49.4	.131	47.1	0.462
35.8	10.3	0.13	51.4	0.443	46.6	0.539	46.6	0.389	46.8	0.590	46.8	1.04	49.4	.145	49.4	.073	49.6	0.392
35.9	13.40	0.13	51.5	0.419	49.1	0.259	49.1	0.355	49.3	0.397	49.3	0.645	51.9	.186	52.0	.119	49.6	0.480
38.3	23.95	0.12	53.9	0.395	49.1	0.306	49.2	0.340	49.3	0.338	49.3	0.748	51.9	.136	52.0	.085	52.1	0.416
38.4	27.2	0.16	54.0	0.306	51.6	0.135	51.6	0.424	51.8	0.161	51.8	0.535	54.4	.204	54.5	.124	52.1	0.390
40.8	31.0	0.14	56.4	0.318	51.6	0.135	51.6	0.416	51.8	0.164	51.8	0.523	54.4	.188	54.5	.057	54.6	0.386
40.9	26.5	0.32	56.4	0.288	54.1	0.160	54.1	0.443	56.7	0.176	54.3	0.481	56.9	.257	56.9	.049	54.6	0.454
40.9	33.4	0.76	58.8	0.266	54.1	0.114	54.1	0.542	54.3	0.057	54.3	0.473	61.8	.224	61.9	.070	57.1	0.490
40.9	33.4	0.18	58.8	0.301	56.6	0.156	56.6	0.608	54.3	0.183	56.8	0.559	64.2	.172	64.3	.038	57.1	0.473
40.9	25.1	0.21	58.8	0.250	61.4	0.193	61.5	0.486	61.7	0.245	61.7	0.744	69.0	.137	69.1	.037	59.6	0.505
43.3	27.8	0.14	61.2	0.295	63.9	0.023	63.9	0.606	64.1	0.214	64.1	0.735	73.8	.100	73.9	.058	62.0	0.500
43.4	26.8	0.17	61.2	0.232	68.7	0.126	68.7	0.442	68.9	0.220	68.9	0.452					62.0	0.606
45.7	19.5	0.13	63.6	0.264	73.4	0.122	73.4	0.511	73.6	0.362	73.7	0.214					64.5	0.541

Table III. (cont.)

Elastic 1+ Level			3.945 MeV 1+ Level		7.03 MeV 2+ Level	
θ cm	dσ/dΩ (mb/sr)	Stat Error (mb/sr)	θ cm	dσ/dΩ (mb/sr)	θ cm	dσ/dΩ (mb/sr)
45.9	16.2	0.09	63.8	0.264	64.5	0.690
48.2	12.4	0.09	66.2	0.260	66.9	0.513
48.3	10.5	0.07	68.4	0.320	69.3	0.508
50.7	10.4	0.09	68.5	0.233	69.3	0.583
50.8	8.91	0.07	70.8	0.233	71.7	0.422
53.1	12.1	0.10	73.1	0.220	74.0	0.428
53.2	11.01	0.08	75.6	0.187		
55.5	13.71	0.09	77.9	0.194		
55.5	15.5	0.12	82.4	0.211		
58.0	17.7	0.19	86.9	0.197		
58.0	14.7	0.10				
58.0	16.7	0.12				
60.4	13.7	0.08				
60.4	16.5	0.10				
62.7	14.6	0.10				
62.9	11.8	0.075				
65.2	8.68	0.065				
66.9	8.37	0.075				
67.6	6.32	0.057				
69.8	4.86	0.051				
72.1	4.07	0.037				
72.1	5.27	0.063				
74.6	3.54	0.035				
76.9	3.14	0.034				
81.3	1.99	0.028				
85.8	0.844	0.019				
116.4	2.76	0.078				
130.1	3.33	0.089				
134.4	3.01	0.084				
138.6	4.79	0.105				
142.7	4.90	0.105				

Table IV. N^{15}.

E_α = 40.5 MeV

Elastic 1/2-			5.276 + 5.304 MeV 5/2+ 1/2+		6.328 MeV 3/2(-)		7.16 MeV (5/2+)		7.31 MeV 3/2+		7.57 MeV (7/2+)		8.31 MeV (1/2+)		8.57 MeV (3/2+)	
θ_{cm}	dσ/dΩ (mb/sr)	Stat. Error (mb/sr)	θ_{cm}	dσ/dΩ (mb/sr)	θ_{cm}	dσ/dΩ (mb/sr)	θ_{cm}	dσ/dΩ (mb/sr)	θ_{cm}	dσ/dΩ (mb/sr)	θ_{cm}	dσ/dΩ (mb/sr)	θ_{cm}	dσ/dΩ (mb/sr)	θ_{cm}	dσ/dΩ (mb/sr)
10.3	4040	12.8	10.54	4.28	10.6	3.71	17.2	0.97	17.3	0.792	17.3	7.50	21.6	0.347	21.6	0.416
12.9	1230	4.97	15.71	6.46	13.2	8.30	21.5	0.591	18.6	1.46	18.6	7.26	23.9	0.403	23.9	0.334
15.4	214	1.13	17.0	5.89	15.8	5.48	23.7	0.562	21.5	1.31	21.5	6.85	26.4	0.217	26.4	0.244
16.7	36.4	0.39	18.29	6.72	18.4	3.92	26.3	0.341	23.7	1.44	23.8	5.84	29.0	0.239	29.0	0.155
17.9	8.19	0.15	21.3	7.33	17.1	3.96	28.8	0.223	26.3	1.20	26.4	4.28	31.6	0.159	31.6	0.086
20.9	128.2	0.46	23.2	7.22	21.4	1.98	34.0	0.063	28.8	0.856	28.9	3.17	34.1	0.164	34.2	0.177
21.6	177.7	1.60	23.4	6.16	23.5	1.06	36.5	0.053	31.5	0.686	31.5	2.54	36.7	0.249	36.7	0.188
22.8	207.2	1.92	26.0	4.11	26.1	0.671	46.6	0.127	34.0	0.661	34.0	2.61	39.3	0.260	39.3	0.207
23.5	200	1.8	28.5	2.47	28.7	0.971	54.0	0.117	36.5	0.976	36.6	2.75	41.8	0.250	41.8	0.140
24.1	196.4	1.77	31.1	1.63	31.2	1.61	56.5	0.084	39.1	1.12	39.1	3.17	44.3	0.324	44.4	0.093
25.4	151.8	1.21	33.2	1.83	33.8	2.02	58.9	0.112	41.6	0.991	41.7	2.80	46.9	0.240	46.9	0.071
25.5	152.4	0.55	36.15	2.42	36.3	1.75	66.1	0.025	44.1	1.14	44.1	3.96	49.3	0.277	49.4	0.062
26.6	121.3	1.09	38.7	2.76	38.9	1.64	68.5	0.063	46.6	0.663	46.7	2.13	51.8	0.237	51.9	0.061
28.0	73.1	0.40	41.2	2.61	41.4	1.09	73.2	0.079	49.1	0.500	49.2	1.67	54.3	0.176	54.4	0.088
30.5	17.15	0.20	43.7	1.98	43.9	0.731	77.8	0.003	51.6	0.495	51.7	1.50	56.8	0.125	56.8	0.053
33.0	2.43	0.079	46.2	1.41	46.4	0.539	82.4	0.033	54.1	0.285	54.1	1.40	59.2	0.072	59.3	0.058
35.5	10.86	0.17	48.65	0.830	48.9	0.531	86.9	0.003	56.5	0.351	56.6	1.16	61.7	0.094	61.8	0.041
38.0	20.6	0.25	51.15	0.714	51.4	0.603	95.6	0.023	59.0	0.307	59.1	1.17	64.1	0.048	64.1	0.034
40.4	20.9	0.26	53.6	0.786	53.75	0.657	99.8	0.252	61.4	0.444	61.5	1.12	66.5	0.033	66.5	0.046
42.9	14.5	0.22	56.0	0.897	56.3	0.633	103.9	0.019	63.8	0.522	63.9	1.06	68.8	0.040	68.9	0.047
45.3	8.32	0.12	58.5	0.941	58.7	0.542			66.2	0.493	66.3	0.923	73.6	0.048	73.7	0.105
47.8	5.85	0.11	60.8	0.921	61.0	0.528			68.6	0.493	68.6	0.876	78.2	0.112	78.3	0.087
50.2	8.02	0.10	63.3	0.773	63.55	0.558			73.3	0.603	73.4	0.835				
52.5	10.9	0.11	65.6	0.645	68.35	0.550			77.9	0.770	78.0	0.798				
55.0	12.5	0.12	67.9	0.680	73.0	0.529			82.4	0.937	82.5	0.737				
57.4	11.85	0.12	72.7	0.896	77.6	0.426			86.9	0.325	87.0	0.377				
59.8	9.99	0.11	77.3	1.04	82.15	0.312			95.6	0.560	95.7	0.628				
62.1	7.02	0.085	81.8	0.824	86.6	0.198			99.8	0.476	99.9	0.409				
64.5	5.10	0.074	86.3	0.598	91.0	0.261			104.0	0.352	104.1	0.619				
66.8	4.27	0.069	90.7	0.619	95.3	0.336										
71.4	2.70	0.057	95.0	0.691	99.5	0.280										
73.7	1.53	0.044	99.2	0.523	103.7	0.222										
80.5	0.720	0.025	103.3	0.645												
84.9	0.128	0.0030														
89.3	0.063	0.0078														
93.5	0.436	0.027														
97.7	0.773	0.036														
101.7	0.816	0.038														

Table V. O^{16}.

E_α = 40.5 MeV

Elastic			6.131 MeV 3- Level		6.916 MeV 2+ Level		7.115 MeV 1- Level		8.870 MeV 2- Level		9.85 MeV 2+ Level		11.08 MeV 3+ Level	
θ_{cm}	$d\sigma/d\Omega$ (mb/sr)	Stat. Error (mb/sr)	θ_{cm}	$d\sigma/d\Omega$ (mb/sr)	θ_{cm}	$d\sigma/d\Omega$ (mb/sr)	θ_{cm}	$d\sigma/d\Omega$ (mb/sr)	θ_{cm}	$d\sigma/d\Omega$ (mb/sr)	θ_{cm}	$d\sigma/d\Omega$ (mb/sr)	θ_{cm}	$d\sigma/d\Omega$ (mb/sr)
15.01	228	1.4	10.2	17.0	17.9	12.1	18.0	1.72	18.1	1.42	18.2	~ 0.3	18.3	~ 1.9
17.50	20.0	0.24	12.8	15.4	20.5	8.23	20.5	2.20	20.7	1.33	20.8	~ 0.3	20.9	~ 1.9
19.99	156	0.78	15.3	17.5	23.0	5.60	23.1	2.37	23.3	1.05	23.4	0.597	23.5	1.88
22.47	251	1.00	17.9	20.3	23.0	5.40	23.1	1.76	25.8	0.900	25.9	0.352	26.1	1.76
22.47	239	2.1	20.4	20.7	25.6	5.68	25.6	1.78	28.4	0.550	28.5	0.290	28.7	1.61
24.95	202	1.2	23.0	17.0	28.1	6.07	28.1	1.15	30.9	0.509	33.6	0.221	33.8	0.945
27.4	92.9	0.65	23.0	15.5	30.6	6.00	30.6	1.06	33.5	0.533	36.2	0.195	36.4	0.734
29.9	19.0	0.21	25.5	11.6	33.2	4.71	33.2	1.55	36.0	0.670	38.7	0.330	38.9	0.707
32.3	1.86	0.07	28.0	6.6	35.7	3.19	35.7	2.21	38.5	0.767	41.2	0.330	41.5	0.636
34.8	15.1	0.21	30.5	5.01	38.2	2.02	38.2	2.62	41.0	0.802	43.7	0.251	44.0	0.563
37.2	26.5	0.29	33.1	5.54	40.7	1.73	40.7	2.65	43.5	0.643	46.2	0.201	46.5	0.374
39.7	24.8	0.27	35.6	6.80	43.1	1.70	43.2	2.19	46.0	0.428	48.7	0.137	49.0	0.423
42.1	13.2	0.21	38.1	7.42	45.6	1.49	45.7	1.66	48.5	0.186	51.2	0.095	51.5	0.355
44.5	4.91	0.13	40.5	7.20	48.0	1.61	48.1	1.15	51.0	0.123	53.7	0.160	54.0	0.352
46.9	4.07	0.12	43.0	5.41	50.5	1.25	50.6	0.90	53.4	0.154	56.1	0.179	56.5	0.283
49.3	9.29	0.19	45.5	3.41	53.0	1.41	53.0	0.50	55.9	0.159	61.0	0.233	61.4	0.236
51.7	15.5	0.26	47.9	2.56	55.4	1.23	55.4	0.45	60.7	0.267	65.8	0.159	66.2	0.188
54.1	17.7	0.28	50.4	2.35	60.2	1.14	60.2	0.34	65.5	0.191	70.5	0.146	70.9	0.068
58.8	11.2	0.23	52.8	2.55	64.9	0.885	65.0	0.53	70.2	0.508				
63.5	5.51	0.16	55.2	2.72	69.6	0.48	69.7	0.63						
68.1	4.67	0.16	60.0	2.43										
			64.7	2.06										
			69.4	1.91										

Table VI. O^{18}.

E_α = 40.5 MeV

Elastic 0+			1.980 MeV 2+		3.55 + 3.63 MeV 4+ 0+		3.92 MeV 2+		4.45 MeV (3+, 1-)		5.09 MeV (3-)		5.25 + 5.33 + 5.37 MeV (2+, 0+, 3+)	
θ_{cm}	dσ/dΩ (mb/sr)	Stat. Error (mb/sr)	θ_{cm}	dσ/dΩ (mb/sr)	θ_{cm}	dσ/dΩ (mb/sr)	θ_{cm}	dσ/dΩ (mb/sr)	θ_{cm}	dσ/dΩ (mb/sr)	θ_{cm}	dσ/dΩ (mb/sr)	θ_{cm}	dσ/dΩ (mb/sr)
9.9	5040	20	10.0	34.0										
12.3	1450	7	12.4	41.1			12.6	7.60						
14.8	240	1.4	14.9	35.0	15.0	3.26	15.0	9.06			15.0	12.5	15.0	2.56
17.2	40	0.4	17.3	19.4	17.4	2.18	17.4	4.16	17.5	0.97	17.5	12.5	17.5	1.18
19.7	173	0.9	19.8	6.37	19.9	2.00	19.9	1.23	19.9	1.19	20.0	10.3	20.0	0.91
22.1	224	0.9	22.2	3.11	22.3	2.02	22.4	1.18	22.4	1.00	22.4	7.18	22.5	0.51
24.5	155	0.8	24.7	6.15	24.8	1.96	24.8	2.30	24.9	0.67	24.9	3.55	24.9	0.78
27.0	54.1	1.2	27.1	8.86	27.2	1.43	27.3	2.68	27.3	0.73	27.4	1.04		
29.4	6.26	0.1	29.5	7.14	29.7	1.05	29.7	1.88	29.7	1.08				
31.8	5.67	0.1	31.9	3.85	32.1	0.82	32.1	1.05	32.2	1.14	32.3	2.10		
34.2	19.5	0.2	34.3	1.40	34.5	0.78	34.6	0.40	34.6	1.00	34.7	2.73		
36.6	23.8	0.2	36.9	1.45	36.9	0.60	37.0	0.45	37.0	0.51	37.1	1.95	37.1	0.47
39.0	18.1	0.1	39.2	2.98	39.3	0.63	39.4	0.73	39.5	0.25	39.5	1.50	39.6	0.42
41.3	8.36	0.09	41.6	3.98	41.7	0.50	41.8	0.90	41.9	0.12	42.0	0.77	42.0	0.31
43.7	2.79	0.05	43.9	3.98	44.1	0.30	44.2	0.79	44.3	0.098	44.4	0.51	44.4	0.22
46.1	3.14	0.06	46.3	3.11	46.5	0.20	46.6	0.48	46.7	0.11	46.7	0.60	46.8	0.14
48.4	5.88	0.08	48.7	1.90	48.9	0.26	49.0	0.23	49.0	0.076	49.1	0.59	49.2	0.19
50.8	6.53	0.03	51.0	1.56	51.2	0.28	51.0	0.22	51.4	0.059	51.5	0.58	51.2	0.23
55.4	5.56	0.06	55.7	2.10	55.9	0.37	56.0	0.34	56.1	0.145	56.2	0.45	56.2	0.054
60.0	2.26	0.04	60.3	1.75										

6.19 MeV ?		6.34 + 6.39 MeV ?		7.12 MeV 4+		7.83 MeV ?		7.96 + 8.04 + 8.08 MeV ?, 1-, ?		8.21 + 8.28 MeV 2+ 3-	
θ_{cm}	dσ/dΩ (mb/sr)	θ_{cm}	dσ/dΩ (mb/sr)	θ_{cm}	dσ/dΩ (mb/sr)	θ_{cm}	dσ/dΩ (mb/sr)	θ_{cm}	dσ/dΩ (mb/sr)	θ_{cm}	dσ/dΩ (mb/sr)
17.6	1.54	17.6	2.82	17.6	2.44	17.7	1.11	17.7	1.55	17.7	4.19
20.1	1.47	20.1	2.30	20.1	1.92	20.2	0.69	20.2	1.73	20.2	2.52
22.5	0.98	22.5	2.08	22.6	1.61	22.7	0.53	22.7	1.86	22.7	1.90
25.0	0.51	25.0	1.63	25.1	1.15	25.1	0.42	25.2	1.34	25.2	1.49
27.5	0.42	27.5	0.96	27.6	0.74	27.6	0.44	27.7	0.80	27.7	1.48
29.9	0.33	29.9	0.83	30.0	0.66	30.1	0.47			30.2	1.17
32.4	0.29	32.4	1.00	32.5	0.67	32.6	0.37	32.6	0.43	32.6	1.17
34.8	0.13	34.8	1.27	34.9	0.69	35.0	0.34	35.1	0.59	35.1	0.91
37.3	0.11	37.3	1.23	37.4	0.60	37.5	0.37	37.5	0.72	37.5	0.32
39.7	0.065	39.7	1.24	39.8	0.52	39.9	0.29	39.9	0.82	40.0	0.42
42.1	0.074	42.1	0.93	42.2	0.37	42.4	0.21	42.4	0.72	42.4	0.42
				44.7	0.28	44.8	0.21	44.8	0.57	44.8	0.42
				47.1	0.31	47.2	0.19	47.2	0.48	47.2	0.37
49.3	0.084			49.5	0.41	49.6	0.18	49.6	0.40	49.7	0.40
51.7	0.094	51.7	0.44	51.9	0.37	52.0	0.22	52.0	0.42	52.1	0.31
		56.4	0.27	56.6	0.34	56.7	0.22	56.8	0.47	56.8	0.32

Table 7. Parameters for optical potential.

Nucleus	-V (MeV)	-W (MeV)	a (fm)	b (fm)
C^{12}	34.44	9.62	0.486	0.700
C^{13}	37.89	10.43	0.519	0.500
N^{14}	35.05	9.48	0.550	0.700
N^{15}	45.09	15.07	0.586	0.500
O^{16}	45.71	15.23	0.606	0.500
O^{18}	46.60	15.70	0.551	0.500

Table 8. Reduced electric quadrupole transition probabilities.

Level	$J\pi$	$B(E2)\downarrow/e^2$ (fm^4)	Other values, comments
C^{12}, 4.433 MeV	2+	13	9.6 fm^4 (Ref. 42)
C^{13}, 3.680 MeV	3/2-	~6	DWBA fit not good.
7.553 MeV	5/2-	~6	DWBA fit not good.
N^{14}, 3.945 MeV	1+	6.5	6.21 ± 0.37 fm^4 (Ref. 43)
7.03 MeV	2+	3.3	3.3 fm^4 (Ref. 43)
N^{15}, 6.328 MeV	3/2-	4.9	
O^{16}, 6.916 MeV	2+	7.7	4.3 ± 1.1 fm^4 (Ref. 44)
O^{18}, 1.980 MeV	2+	8.4	7.2 ± 0.14 fm^4 (Ref. 45) 8.0 ± 3.6 fm^4 (Ref. 46)
3.92 MeV	2+	3.0	$0.16^{+0.014}_{-0.009}$ fm^4 (Ref. 47)

Table 9. Reduced electric octupole transition probabilities.

Level	Jπ	$B(E3)\downarrow/e^2$ (fm^6)	Other values, comments
C^{12}, 9.64 MeV	3-	50 - 70	DWBA fit poor
N^{14}, 5.10 MeV	2-	40	104 ± 21 fm^6 (Ref. 43)
5.83 MeV	3-	60	108 ± 6 fm^6 (Ref. 43)
N^{15}, 5.276 MeV	5/2+	60	
7.57 MeV	7/2+	60	
O^{16}, 6.131 MeV	3-	90	210^{+25}_{-16} fm^6 (Ref. 37)
O^{18}, 5.09 MeV	3-	40	

FIG. 1

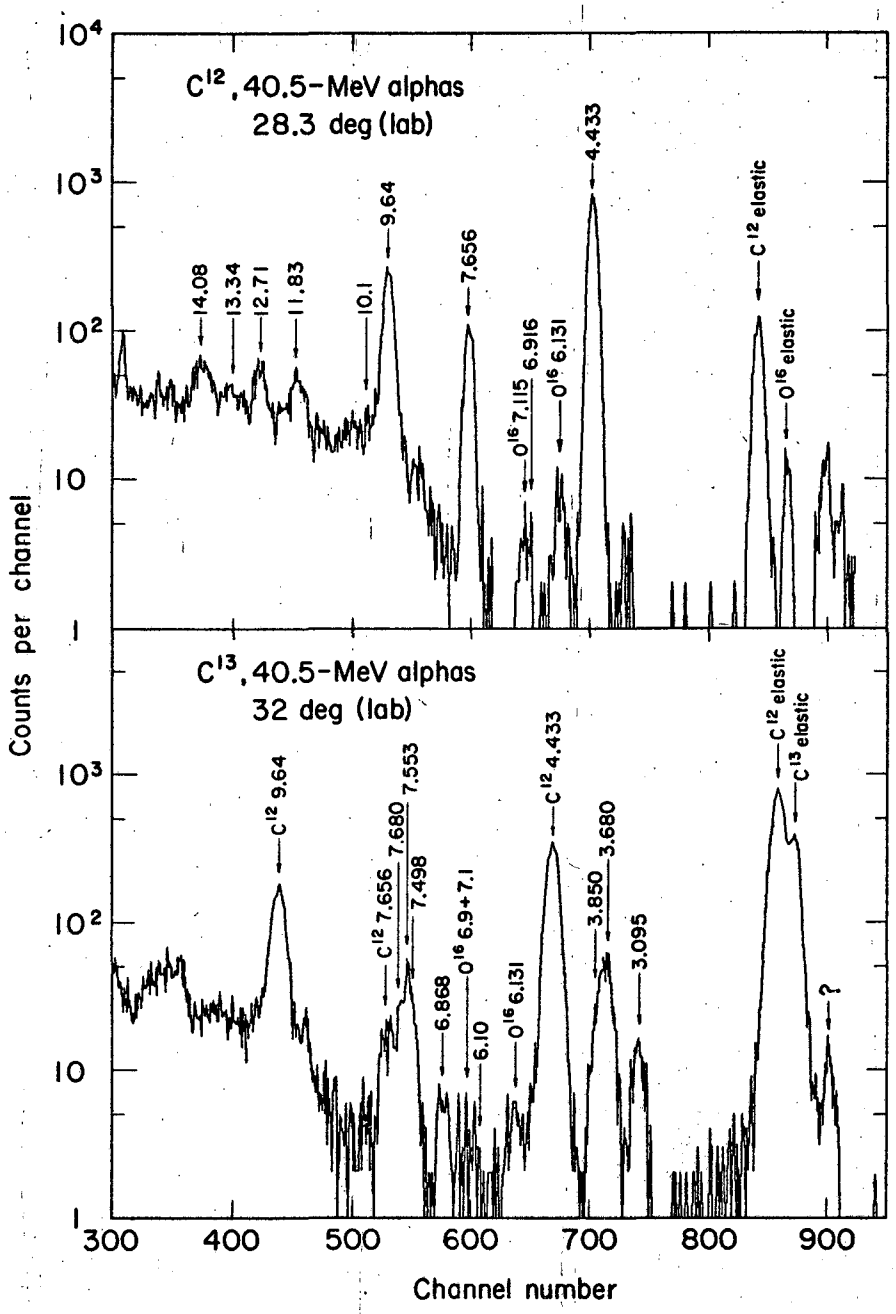

MUB-7223

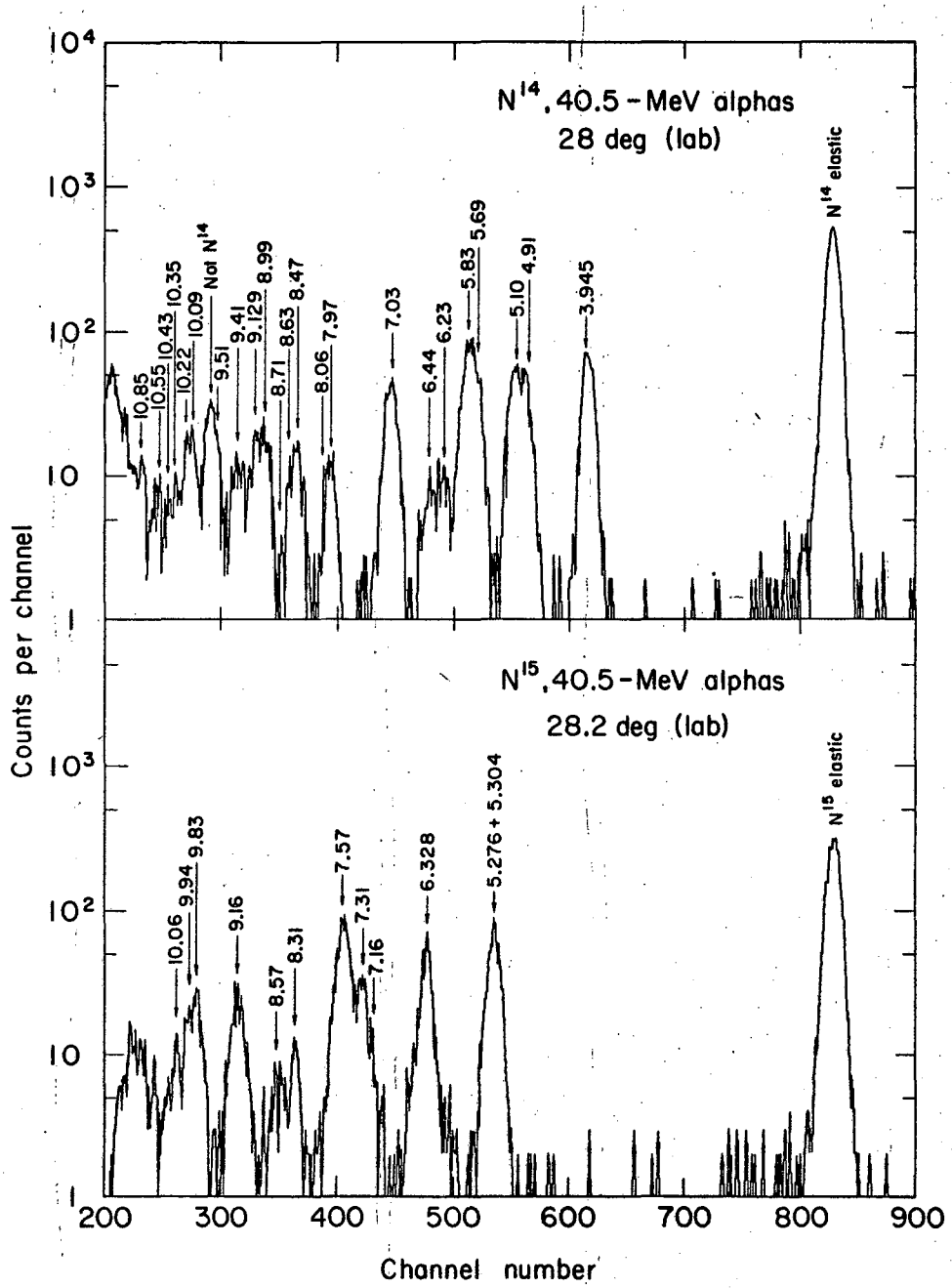
N14, 40.5-MeV alphas
28 deg (lab)
N14 elastic
10.85
10.55
10.43
10.35
10.22
10.09
Nat N14
9.51
9.41
9.129
8.99
8.71
8.63
8.47
8.06
7.97
7.03
6.44
6.23
5.83
5.69
5.10
4.91
3.945
N15, 40.5-MeV alphas
28.2 deg (lab)
N15 elastic
10.06
9.94
9.83
9.16
8.57
8.31
7.57
7.31
7.16
6.328
5.276 + 5.304
Counts per channel
Channel number
MUB-7224

FIG. 3

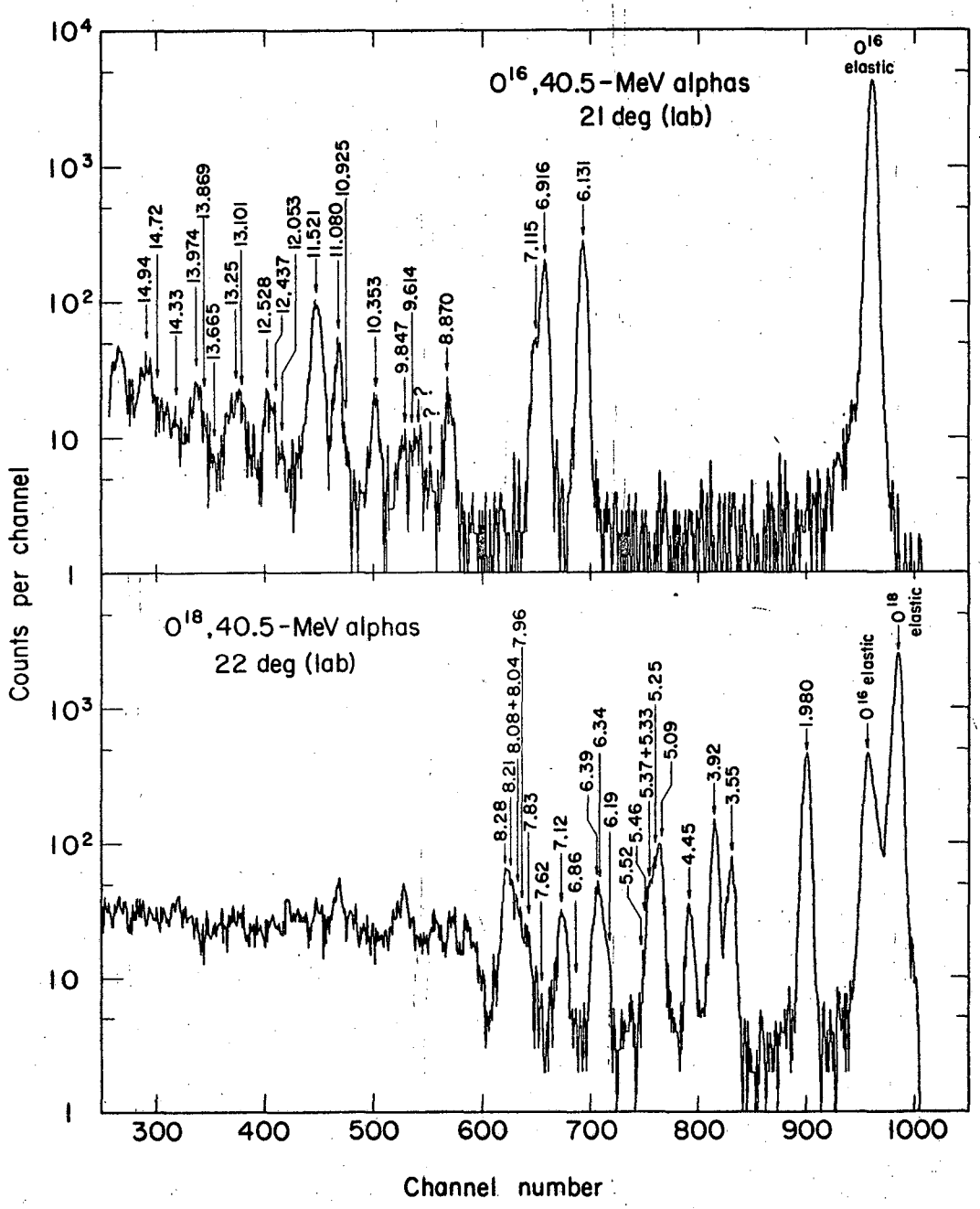

MUB-7225

C12

FIG. 4

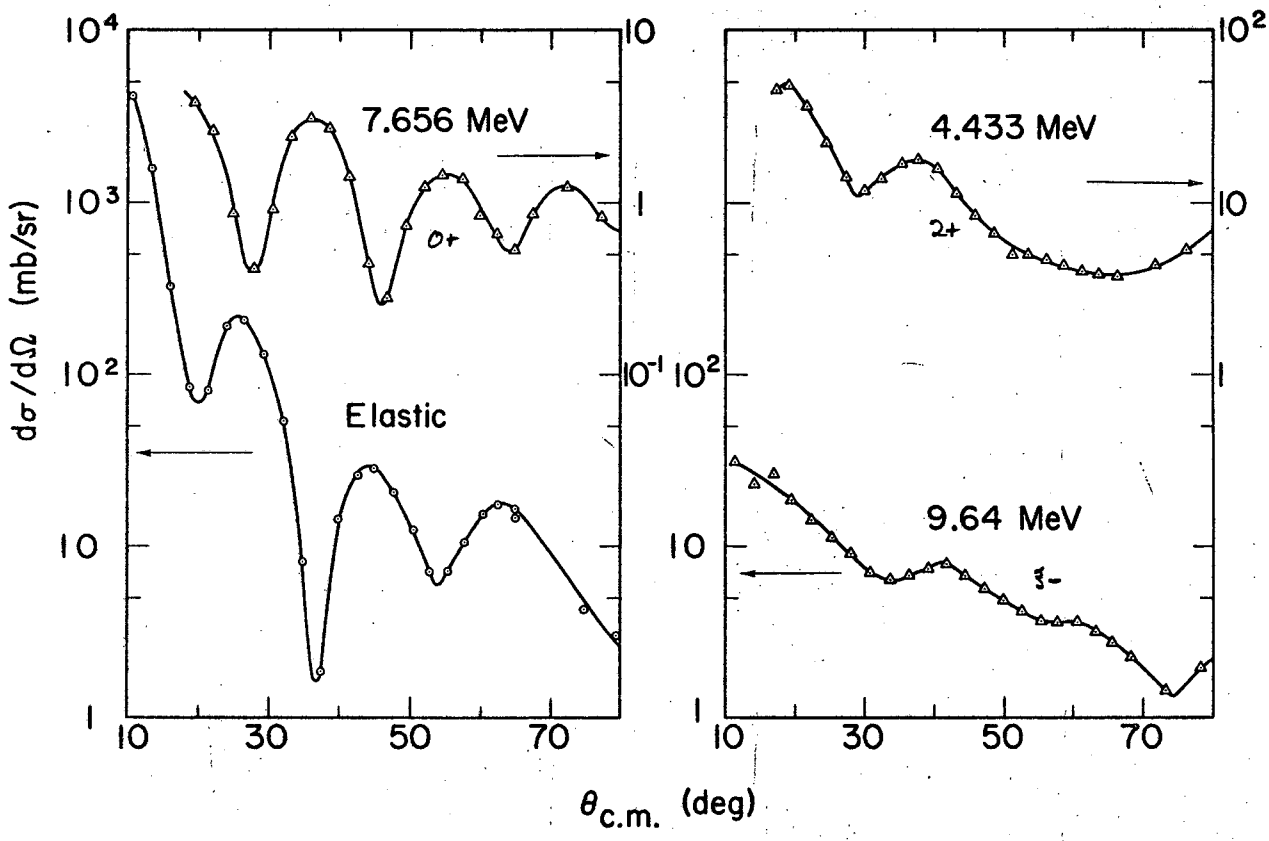

MUB-7226

FIG 5

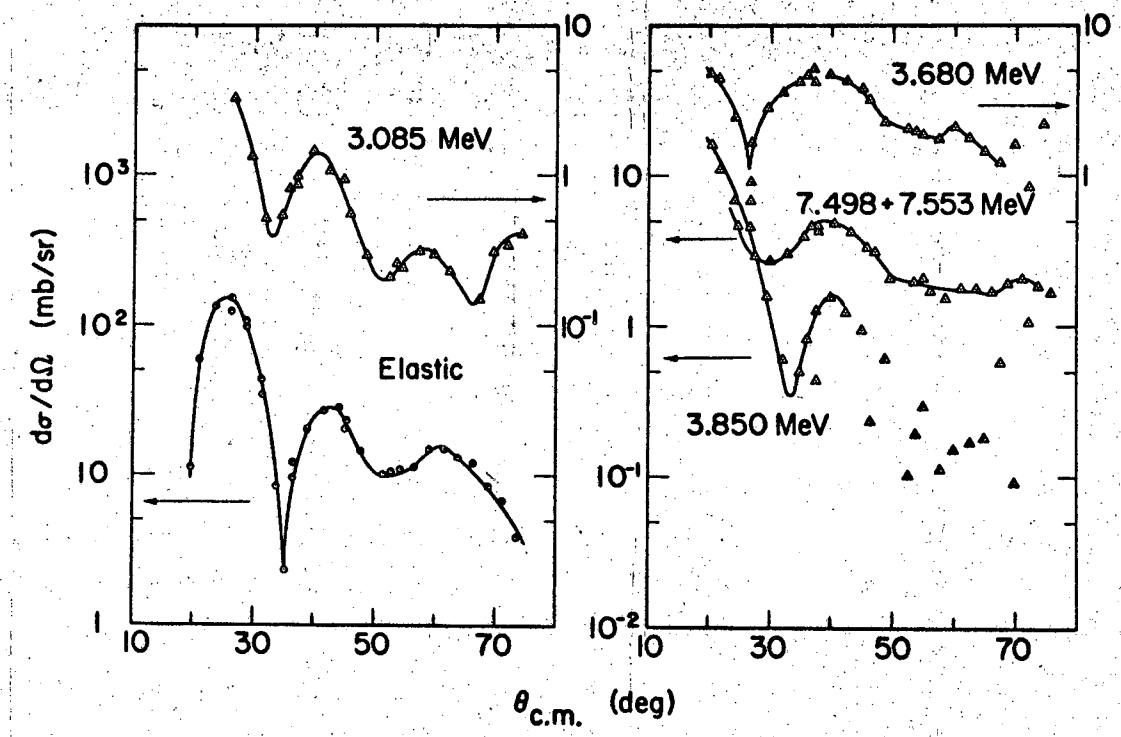
3.085 MeV
Elastic
3.680 MeV
7.498 + 7.553 MeV
3.850 MeV
dσ/dΩ (mb/sr)
θc.m. (deg)
MUB-7227

FIG. 6

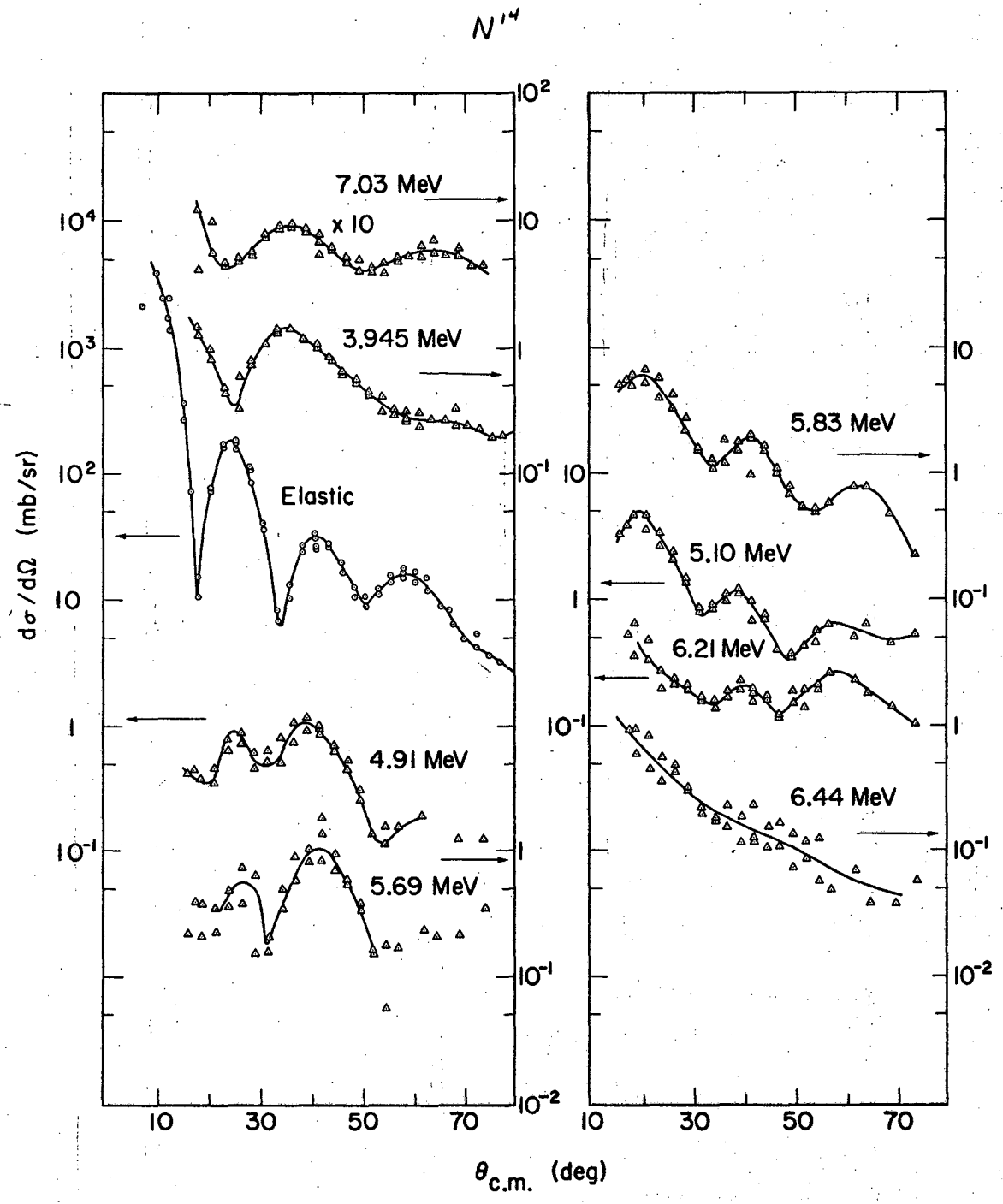

MUB-7228

FIG. 7

N^{15}

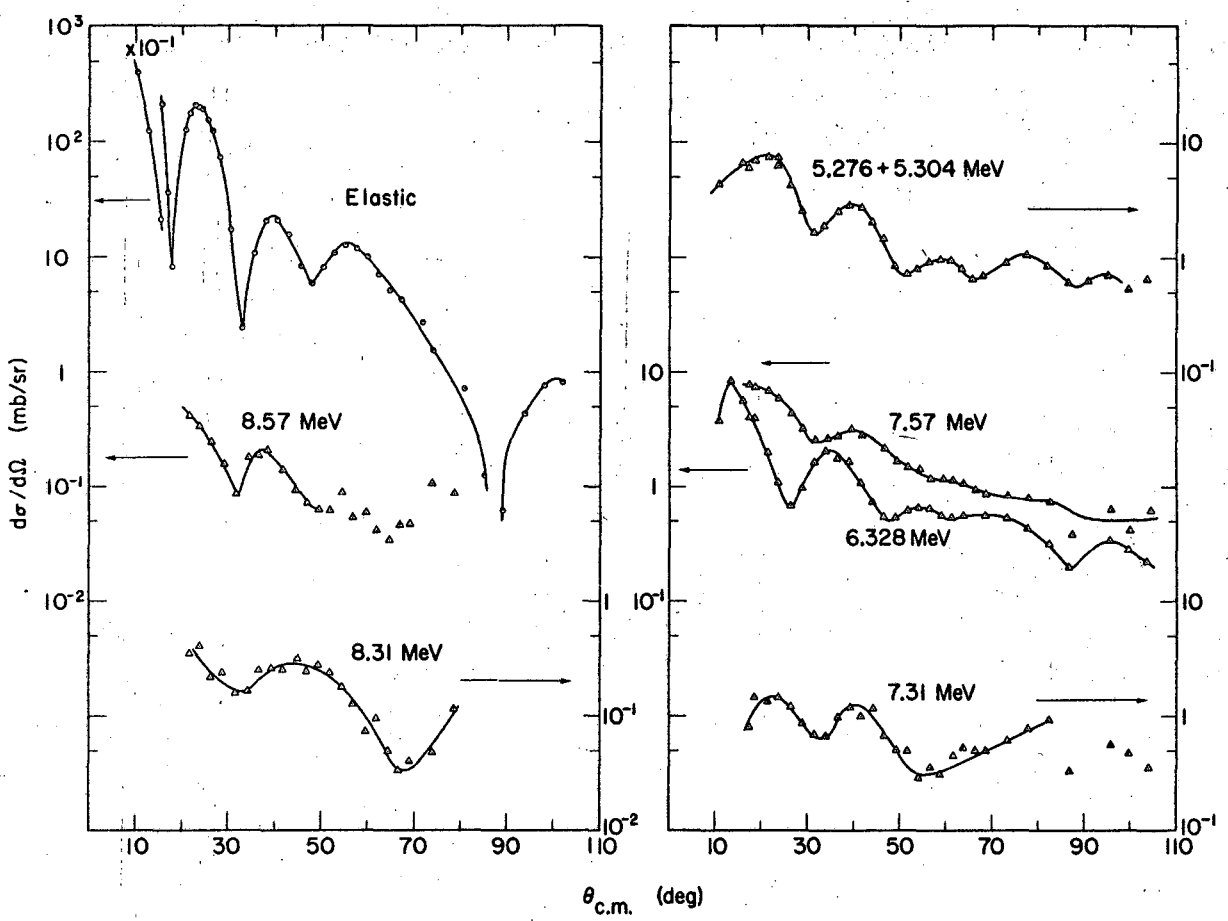
x10⁻¹
Elastic
8.57 MeV
8.31 MeV
5.276 + 5.304 MeV
7.57 MeV
6.328 MeV
7.31 MeV
dσ/dΩ (mb/sr)
θc.m. (deg)

FIG. 8

O^{16}

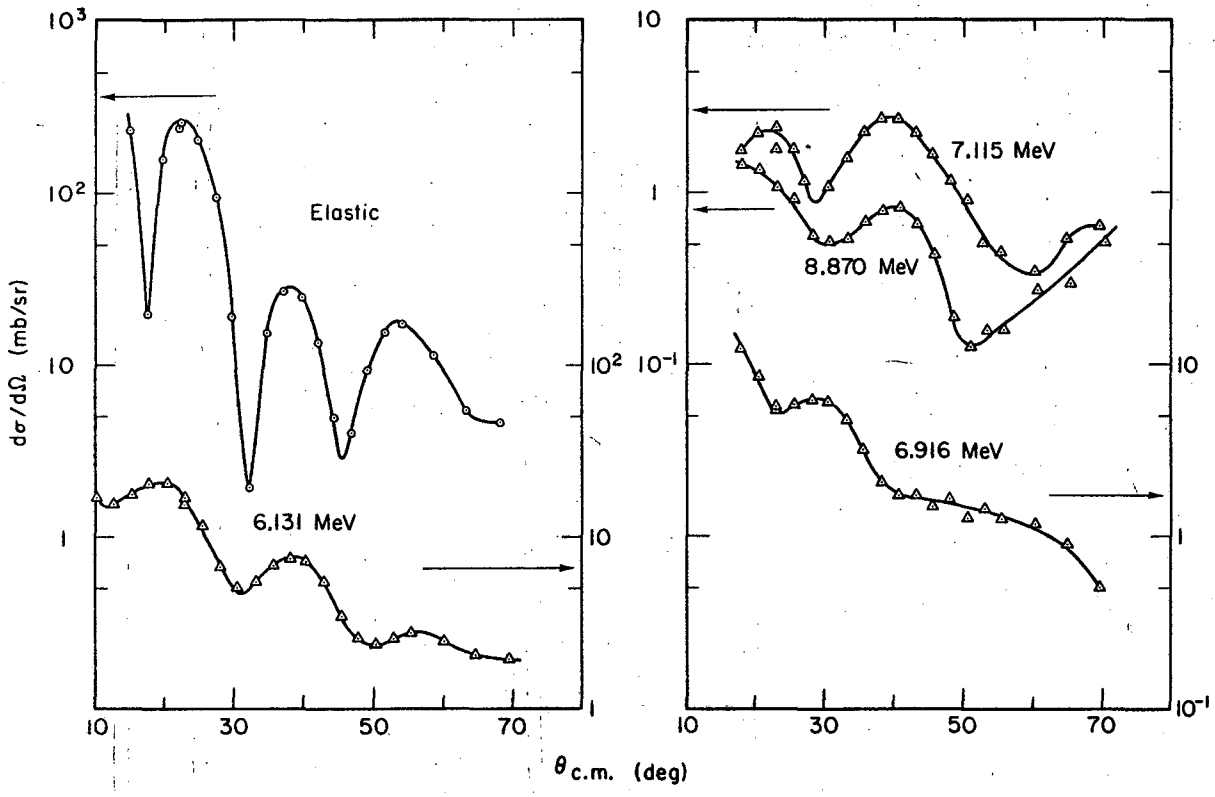

MUB-7230

FIG. 9

O^{18}

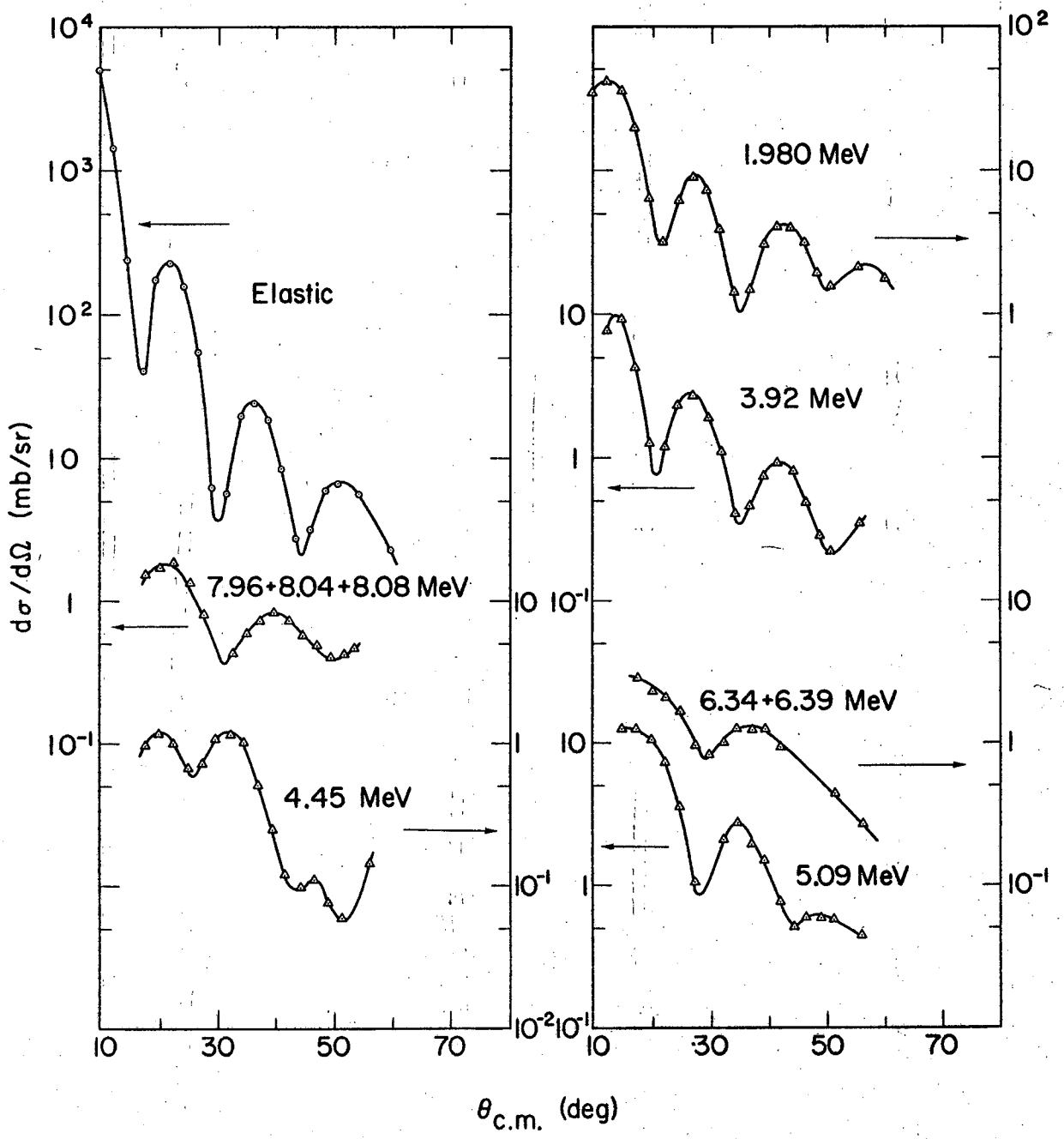

MUB-7231

FIG. 10

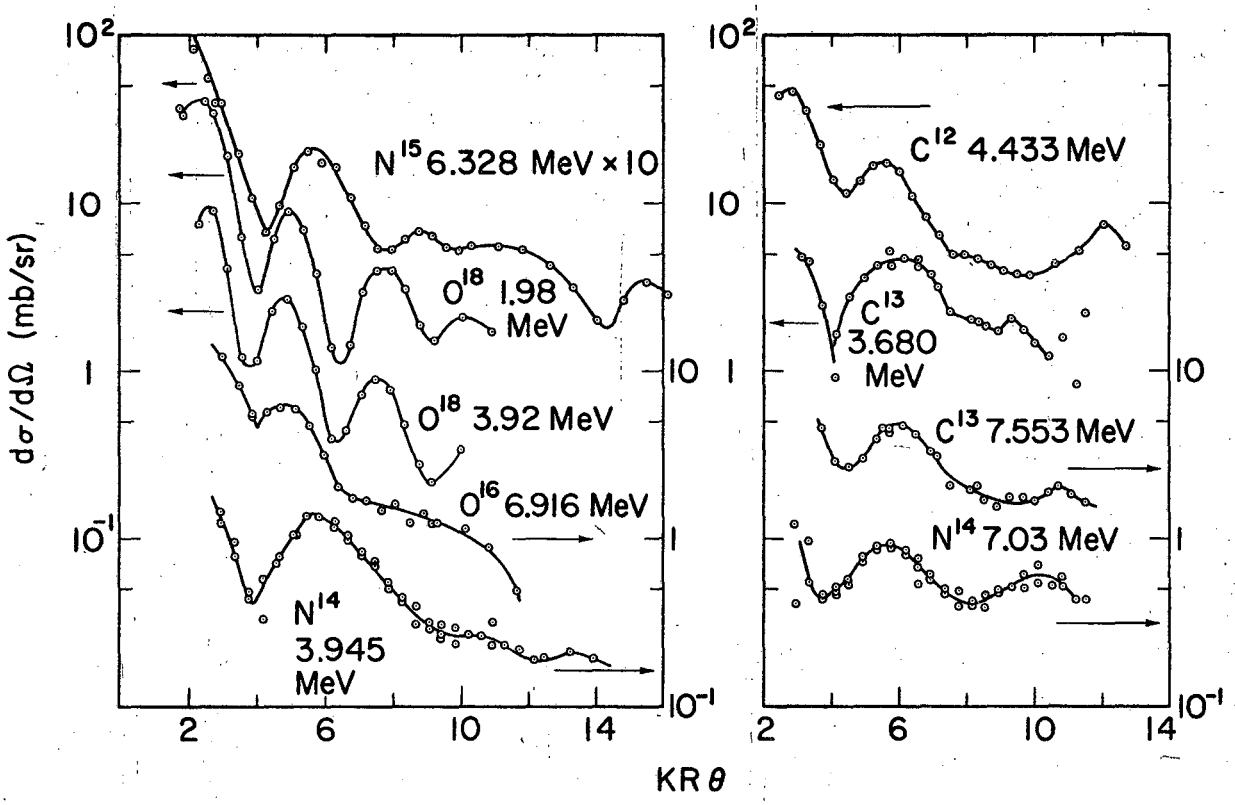

MUB-7232

FIG. 11

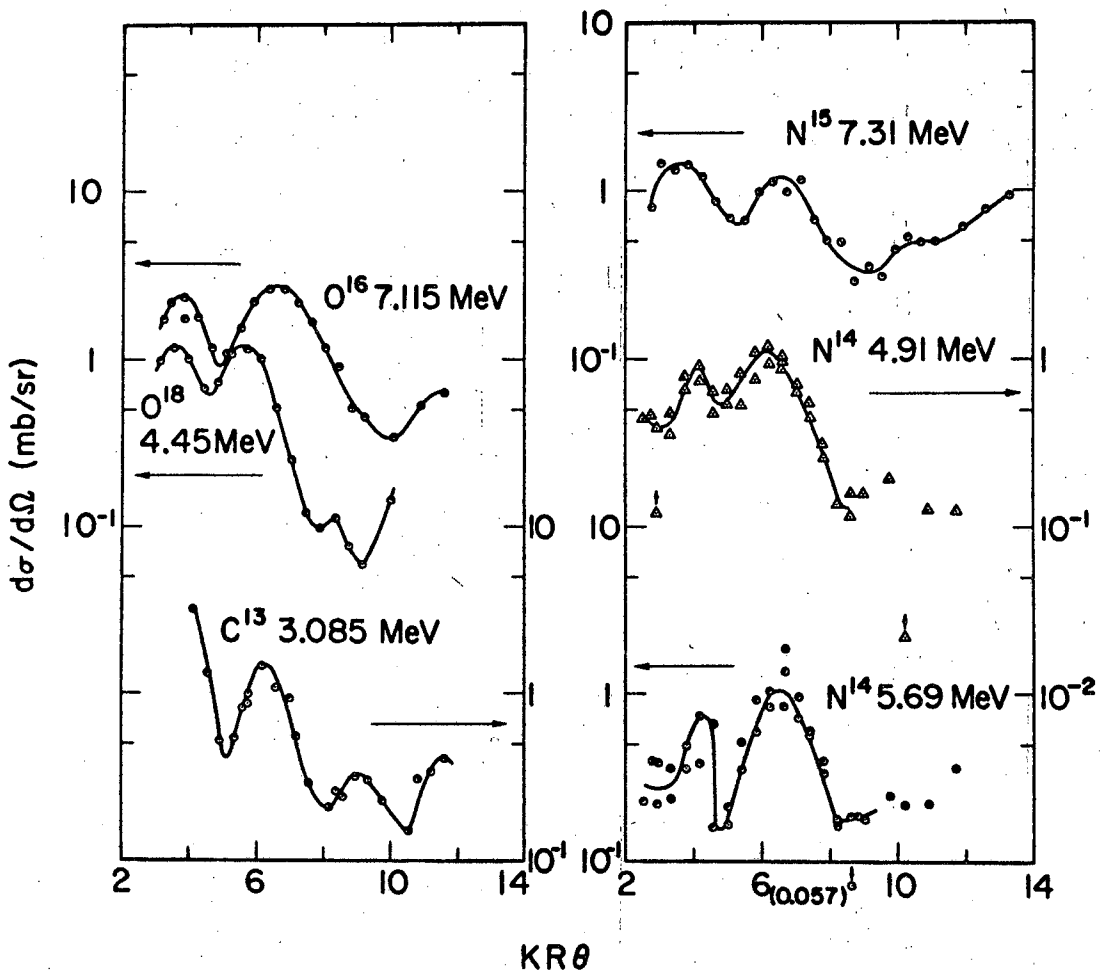

MUB-7233

FIG. 12

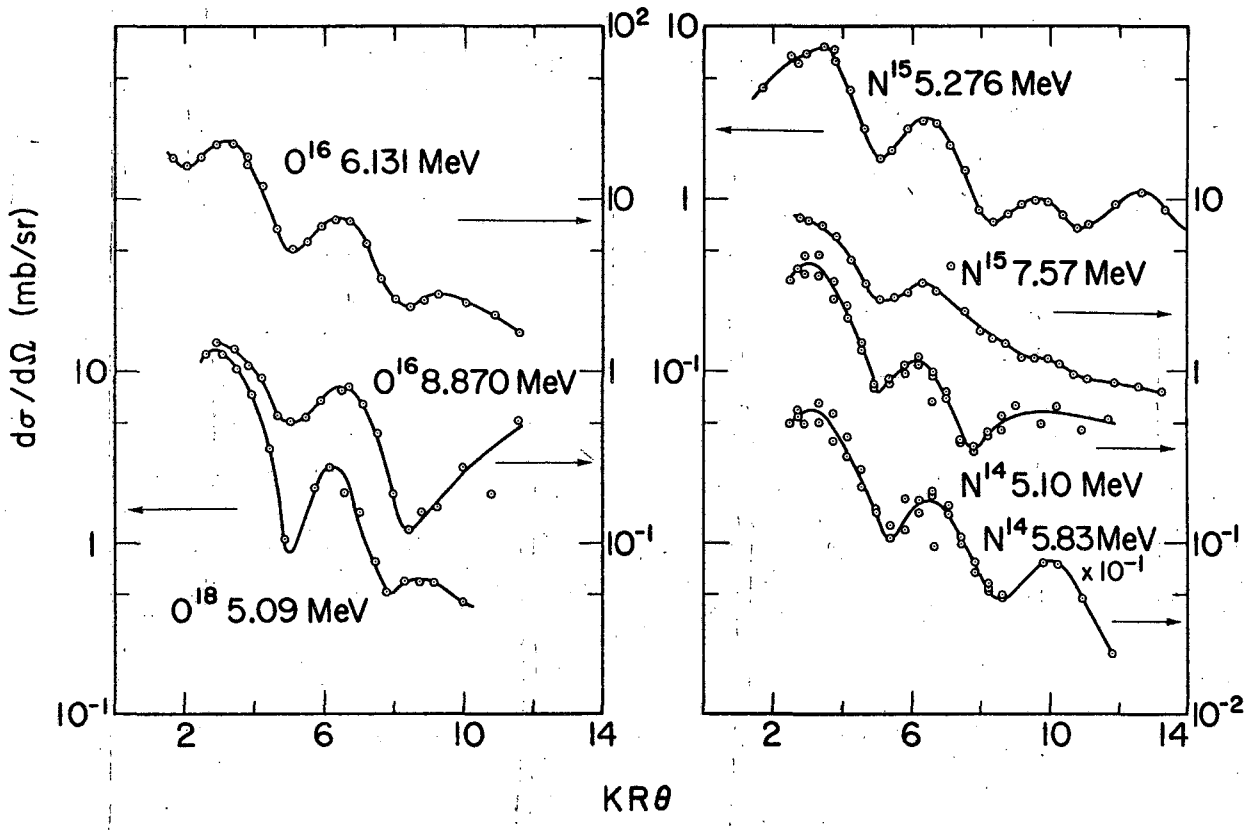

MUB-7234

FIG. 13

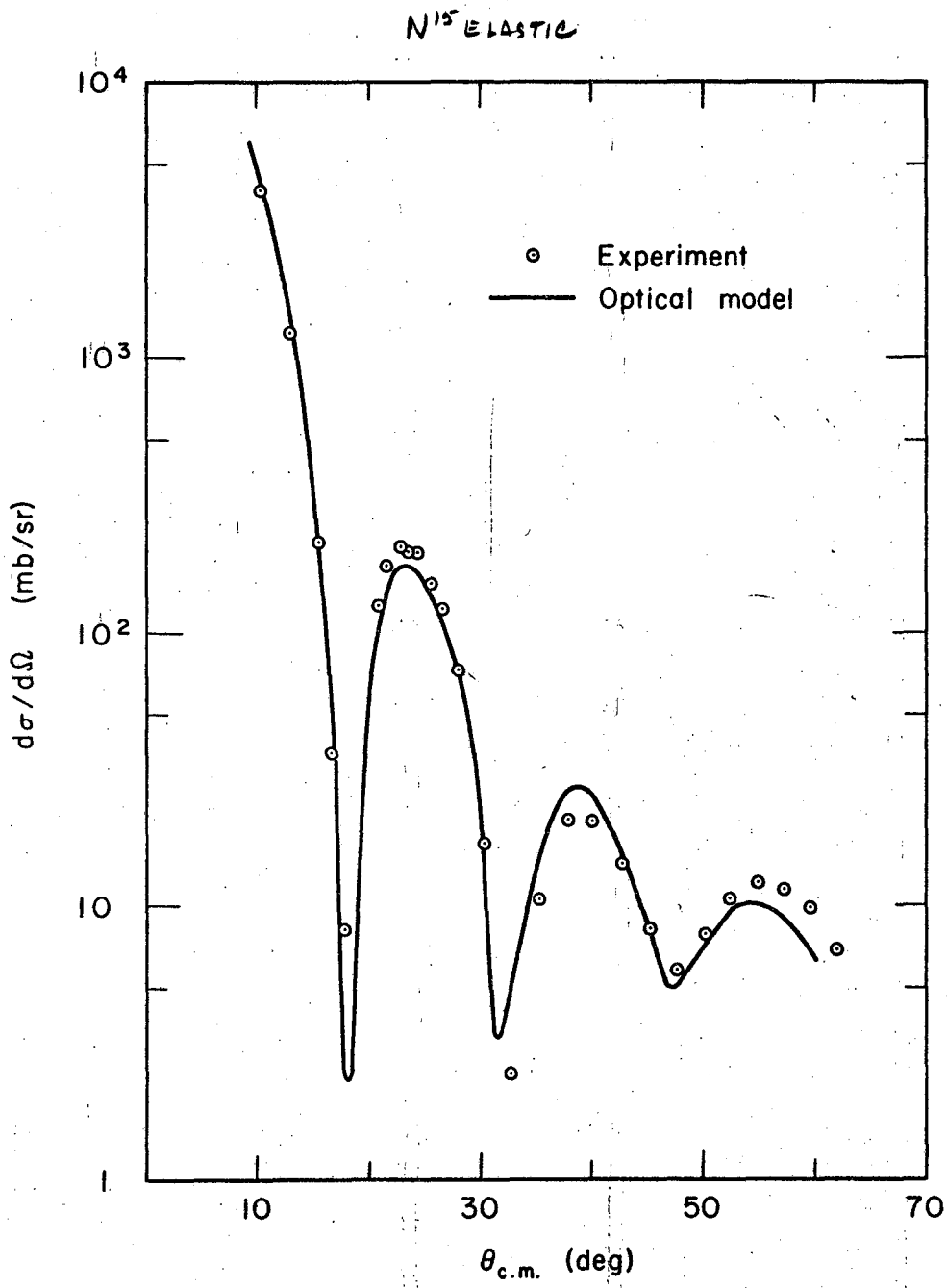

MUB-7238

FIG 14

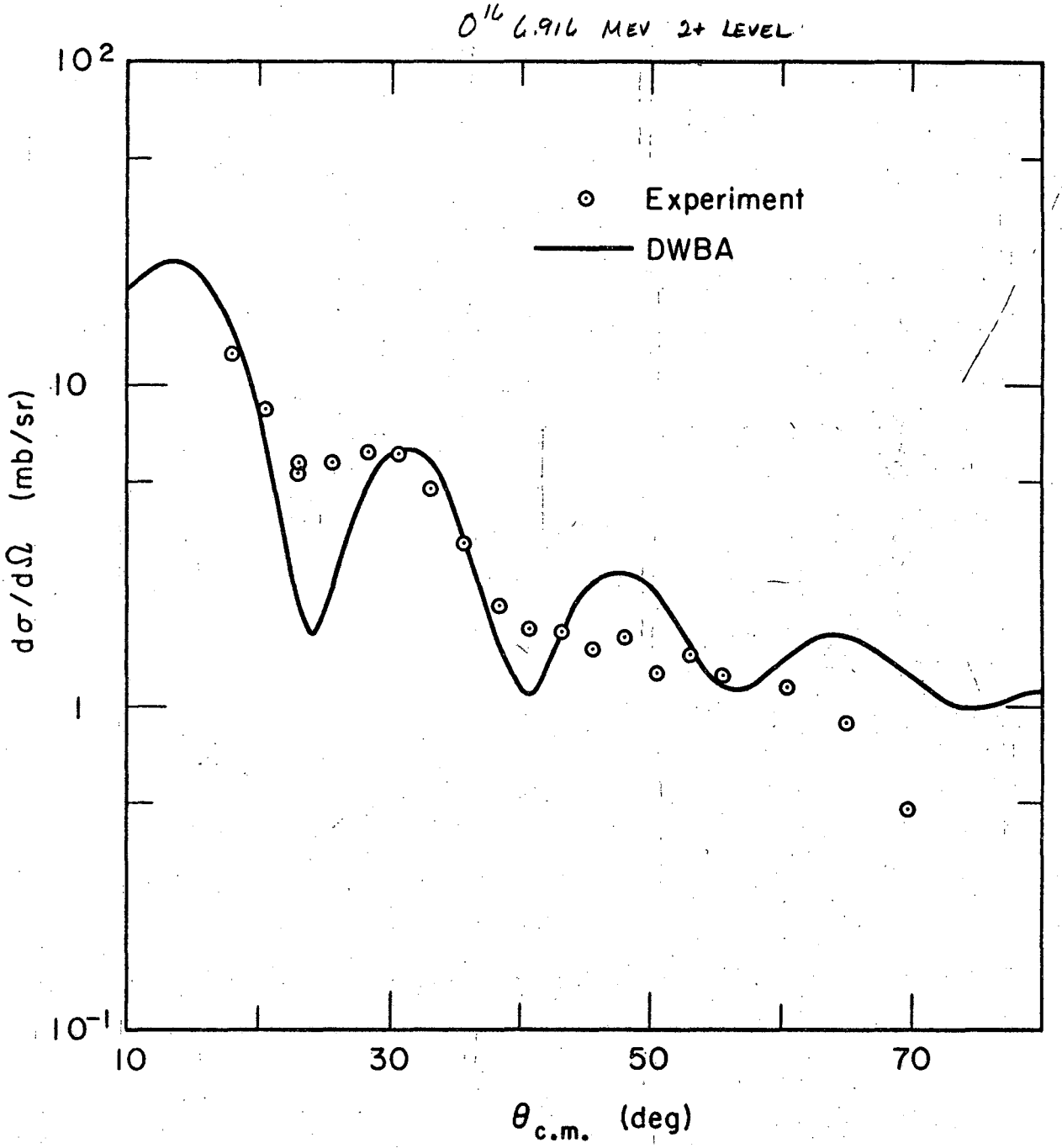

MUB-7250

FIG. 15

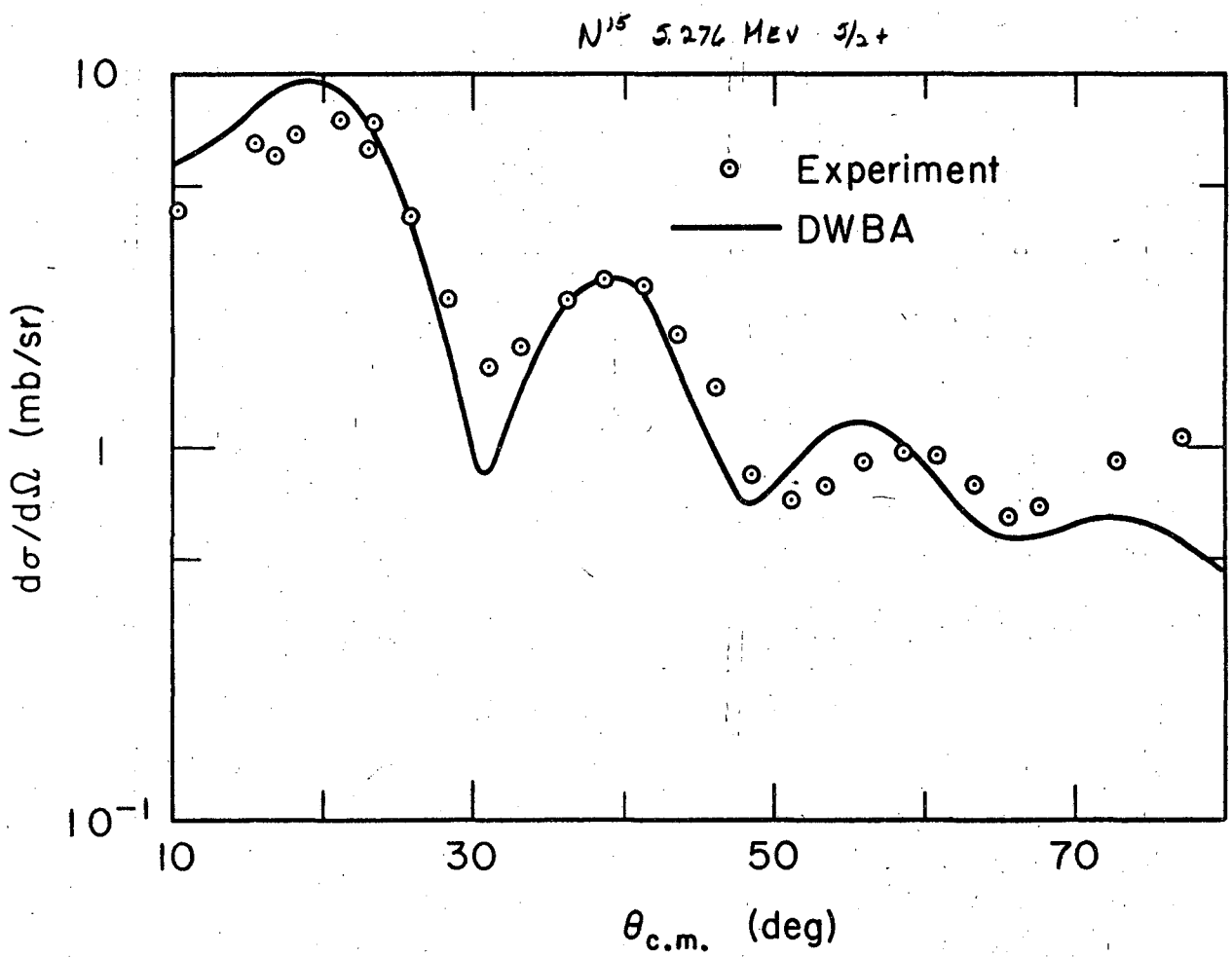

MUB-7256

This report was prepared as an account of Government sponsored work. Neither the United States, nor the Commission, nor any person acting on behalf of the Commission:

A. Makes any warranty or representation, expressed or implied, with respect to the accuracy, completeness, or usefulness of the information contained in this report, or that the use of any information, apparatus, method, or process disclosed in this report may not infringe privately owned rights; or

B. Assumes any liabilities with respect to the use of, or for damages resulting from the use of any information, apparatus, method, or process disclosed in this report.

As used in the above, "person acting on behalf of the Commission" includes any employee or contractor of the Commission, or employee of such contractor, to the extent that such employee or contractor of the Commission, or employee of such contractor prepares, disseminates, or provides access to, any information pursuant to his employment or contract with the Commission, or his employment with such contractor.